# Expression of *E. coli* glycogen branching enzyme in an *Arabidopsis* mutant devoid of endogenous starch branching enzymes induces the synthesis of starch-like polyglucans

**Running Title:** Synthesis of starch-like polyglucans by *E. coli* BE

Laura Boyer [1], Xavier Roussel [1], Adeline Courseaux [1], Ofilia Mvundza Ndjindji [2,3], Christine Lancelon-Pin [2,3], Jean-Luc Putaux [2,3], Ian Tetlow [4], Michael Emes [4], Bruno Pontoire [5], Christophe D'Hulst [1] and Fabrice Wattebled [1, *]

[1] Univ. Lille, UGSF, Unité de Glycobiologie Structurale et Fonctionnelle, UMR8576 CNRS –, F-59000 Lille, France

[2] Université Grenoble Alpes, Centre de Recherches sur les Macromolécules Végétales (CERMAV), F-38000 Grenoble, France

[3] CNRS, CERMAV, F-38000 Grenoble, France

[4] Department of Molecular and Cellular Biology, Science Complex, University of Guelph, Guelph, Ontario N1G 2W1, Canada

[5] UR1268 BIA, INRA, F-44300 Nantes, France

[*] Corresponding author: fabrice.wattebled@univ-lille1.fr

Total word count: 7707

**ABSTRACT**

Starch synthesis requires several enzymatic activities including branching enzymes (BEs) responsible for the formation of α(1→6) linkages. Distribution and number of these linkages are further controlled by debranching enzymes (DBEs) that cleave some of them, rendering the polyglucan water-insoluble and semi-crystalline. Although the activity of BEs and DBEs is mandatory to sustain normal starch synthesis, the relative importance of each in the establishment of the plant storage polyglucan (i.e. water-insolubility, crystallinity, presence of amylose) is still debated. Here, we have substituted the activity of BEs in *Arabidopsis* with that of the *Escherichia coli* glycogen branching enzyme (GlgB). The latter is the BE counterpart in the metabolism of glycogen, a highly branched water-soluble and amorphous storage polyglucan. GlgB was expressed in the *be2 be3* double mutant of *Arabidopsis* that is devoid of BE activity and consequently free of starch. The synthesis of a water-insoluble, partly crystalline, amylose-containing starch-like polyglucan was restored in GlgB-expressing plants, suggesting that BEs origin only have a limited impact on establishing essential characteristics of starch. Moreover, the balance between branching and debranching is crucial for the synthesis of starch, as an excess of branching activity results in the formation of highly branched, water-soluble, poorly crystalline polyglucan.

**KEYWORDS**

Starch, glycogen, α-glucan, polyglucan, branching enzyme, GlgB, *Arabidopsis thaliana*, *Escherichia coli*, debranching enzyme.

46 **INTRODUCTION**

47 Amylopectin is one of the two homopolymers of glucose that constitute native starch
48 in plants and algae. Like glycogen found in bacteria, fungi and animals it is composed of
49 glucosyl residues linked by α(1→4) O-glycosidic bonds and branched through α(1→6)
50 linkages. However, the degree of branching of amylopectin does not exceed 5-6%, while it
51 usually reaches 8 to 10% in glycogen (Buleon *et al.*, 1998, Roach *et al.*, 2012). Moreover,
52 the distribution of α(1→6) linkages is different in both polyglucans. On the one hand, in
53 glycogen, branch points are regularly distributed in the macromolecule, leading to the
54 formation of a spherical homogenous structure with limited size (Melendez-Hevia *et al.*,
55 1993). On the other hand, amylopectin exhibits a heterogeneous molecular organization in
56 which short linear segments are clustered and branch points form amorphous lamellae.
57 Since the initial proposition of cluster organization of amylopectin (French, 1972, Robin *et*
58 *al.*, 1974), several models of cluster pattern have been proposed (Bertoft, 2013). Hizukuri's
59 model suggests that clusters follow one another linearly. The clusters are linked together by
60 longer glucans that expand from the preceding structure to the following (Hizukuri, 1986).
61 More recently, Bertoft has proposed an alternative model in which clusters are linked side
62 by side to a long, linear, glucan backbone (Bertoft, 2004). In Bertoft's model, the formation
63 of a new cluster does not depend on the synthesis of a previous one. Regardless of which
64 amylopectin model is considered, these differences between amylopectin and glycogen lead
65 to different properties for both polymers. Amylopectin is water-insoluble and partly
66 crystalline whereas glycogen is water-soluble and amorphous.

67 The biosynthesis of these polysaccharides involves the same set of enzymatic
68 activities:

69 i. Polymerizing enzymes (i.e. starch- or glycogen-synthases) that transfer the glucose
70 moiety of a nucleotide-sugar (being ADP-glucose or UDP-glucose) to the non-
71 reducing end of an α-glucan by creating α(1→4) linkages (Fujita *et al.*, 2012).

72 ii. Branching enzymes (1,4-α-glucan:1,4-α-glucan 6-glucosyltransferase; EC 2.4.1.18)
73 that introduce the α(1→6) branch points by rearranging linear glucans. These
74 enzymes cleave an α(1→4) linkage and then transfer the released glucan in

75 α(1→6) position by an intermolecular or intramolecular mechanism (Tetlow,
76 2012).
77 However, about 20 years ago, it was suggested that isoamylase-type debranching
78 enzymes (DBEs) were required for the building of the final structure of amylopectin in
79 plants, determining insolubility and partial crystallization (Ball *et al.*, 1996, Mouille *et al.*,
80 1996, Myers *et al.*, 2000). This idea was further supported and confirmed by several studies
81 conducted with different plant species (James *et al.*, 1995, Nakamura, 1996, Rahman *et al.*,
82 1998, Delatte *et al.*, 2005, Wattebled *et al.*, 2005). In all cases, the lack of isoamylase-type
83 DBEs (except the ISA3 isoform dedicated to starch degradation) caused a strong reduction
84 of starch accumulation, and a modification of the ultrastructure of the residual starch
85 accompanied by a decrease of the crystallinity index. Moreover, these isoamylase mutants
86 also accumulate phytoglycogen, a water-soluble and amorphous glucan structure, which is
87 comparable to that of the glycogen found in animals, fungi and bacteria. Compared to wild-
88 type starch, phytoglycogen displays significant modifications of chain length distribution
89 characterized by enrichment in very short chains (DP 3-5). The crystallization of starch
90 clearly depends on the distribution of α(1→6) linkages, but also on chain length
91 distribution (Pfister *et al.*, 2014). Starch synthases (by elongating glucans) and isoamylases
92 (by removing some branch points) are key enzymes that control both parameters that are
93 crucial to define the final structure and properties of starch. Modification of plant branching
94 enzyme (BE) activity level can affect the physicochemical characteristics of starch as well.
95 For instance, the reduction of BE activity in potato by the antisense inhibition of both SBE
96 A and SBE B isoforms induces the synthesis of very-high-amylose starch in potato tubers
97 (Schwall *et al.*, 2000). In rice and maize, modification of BE activity (by mutation or over-
98 expression) alters the structure and properties of the endosperm starch (Satoh *et al.*, 2003,
99 Tanaka *et al.*, 2004, Yao *et al.*, 2004). Although it is obvious that BEs are mandatory for
100 the synthesis of starch since these enzymes are the only one that create the α(1→6)
101 linkages, their actual contribution for the determination of starch characteristics (i.e. water-
102 insolubility, semi-crystallinity, presence of amylose, amylopectin $DP_{max}$ at 12-13) has not
103 been precisely evaluated so far. Recently, the synthesis of high amounts of insoluble
104 polyglucans was reported in a quintuple mutant of Arabidopsis lacking all four DBEs plus

105 one form of plastidial α-amylase (Streb *et al.*, 2008). Thus, the necessity of DBEs *per se* for
106 the determination of the water-insolubility and crystallinity of starch could be questioned,
107 although the polyglucans synthesized in the above-mentioned quintuple mutant displays
108 specific features (very high DP<10 content for instance) not observed in WT starch.
109 Therefore, the function of BEs appears to be crucial in establishing the intrinsic structural
110 features of starch although crystallinity of the polyglucan synthesized in the Arabidopsis
111 quintuple mutant was not reported in (Streb *et al.*, 2008). Branching enzymes are classified
112 into two groups depending on their amino-acid sequences: group I or B-family and group II
113 or A-family (Burton *et al.*, 1995). The *in vitro* determination of catalytic parameters
114 showed that BEI is more active on amylose than amylopectin, in contrast to the members of
115 the BEII group (Guan *et al.*, 1993, Guan *et al.*, 1994). Moreover, BEI transfers longer
116 glucans compared to BEII (Guan *et al.*, 1997). GlgB that generates α(1→6) linkages during
117 glycogen synthesis has catalytic properties obviously distinct to that of maize BEII and BEI
118 (Guan *et al.*, 1997).

119 In this work, our objective was to test whether the phylogenetic and family origin of
120 BEs was crucial for the production of water-insoluble semi-crystalline polysaccharides. The
121 expression of maize BEI or BEII or both BEI and BEII in a *glgB*- mutant of *E. coli* resulted
122 in the synthesis of glycogen-like but not starch-like polysaccharides (Guan *et al.*, 1995).
123 Similar results were obtained after the expression of maize BEIIa and/or BEIIb in a
124 branching enzyme mutant of yeast (Seo *et al.*, 2002). Alternatively, *E. coli* glycogen
125 branching enzyme (GlgB) was already expressed in different plants such as potato
126 (Kortstee *et al.*, 1996, Huang *et al.*, 2013) and rice (Kim *et al.*, 2005) leading to
127 modification of the structure of the synthesized polyglucans (increased branching degree
128 and altered chain length distribution of amylopectin). However in both cases, the
129 endogenous BEs were still active, thus preventing from the determination of the specific
130 contribution of GlgB for the synthesis of starch.

131 Arabidopsis contains only two BEs involved in transitory starch synthesis and both of
132 them belong to the BEII group (Fisher *et al.*, 1996). Arabidopsis *be2 be3* double mutants
133 are unable to create branch points during polysaccharide synthesis and are therefore
134 starchless (Dumez *et al.*, 2006). We used these plants, devoid of endogenous BEs, to

135 express the *E. coli* GlgB glycogen branching enzyme to evaluate whether enzyme
136 metabolic origin (i.e. glycogen versus starch) can sustain the synthesis of starch-like
137 polyglucan. More precisely, a starch-like polyglucan could be defined as a polyglucan that
138 is water-insoluble, partly crystalline, contain both amylopectin and amylose and in which
139 amylopectin $DP_{max}$ is 12-13. GlgB is involved in the synthesis of glycogen and belongs to
140 the BEI family (Sawada *et al.*, 2014). The analysis of polyglucan accumulation in
141 *Arabidopsis* plants expressing GlgB revealed that the balance between branching and
142 debranching activities, assuming that elongating activity is not-limiting, establishes the
143 structure of the polysaccharide produced, regardless of the origin of the branching enzyme.
144
145 **MATERIALS AND METHODS**
146
147 *Cloning of the glycogen branching enzyme (GlgB) of* Escherichia coli
148 The chloroplast transit peptide of *Arabidopsis thaliana* Branching Enzyme 2
149 (At5g03650) was identified with the use of ChloroP 1.1
150 (http://www.cbs.dtu.dk/services/ChloroP/). The corresponding nucleotide sequence was
151 reconstituted by PCR using two long and partially complementary primers, TPbe2-1 and
152 TPbe2-2 (primer sequences and method of amplification are depicted in details in Figure
153 S1). A fragment corresponding to the first 30 nucleotides of the 5' end of *glgB* was then
154 added downstream of the sequence encoding the transit peptide (Figure S1). In parallel, the
155 coding sequence of *glgB* was amplified by PCR from genomic DNA of *E. coli* TOP10
156 using primers glgB-For and glgB-Rev (Figure S1). The final sequence was obtained after
157 20 cycles of polymerase extension of both overlapping sequences. This chimeric cDNA
158 was subsequently amplified by PCR with primers TPbe2 for-CACC and glgB rev (Figure
159 S1) and cloned into pENTR™/D-TOPO prior to be transferred by homologous
160 recombination into pMDC32 using the gateway® technology (Life Technologies). The
161 sequence was checked by full-sequencing before further uses. All PCR reactions were
162 performed using a high-fidelity DNA polymerase (Kapa Hifi from KAPABIOSYSTEM®).
163
164 *Plant growth, transformation and selection*

165 Unless otherwise indicated, Arabidopsis plants were cultivated in growth cabinet in
166 16-h light : 8-h dark regime at 23°C during the day and 20°C during the night under 75%
167 relative humidity and 100 $\mu E.m^{-2}.s^{-1}$ irradiance.
168 The *be2 be3* double mutant of *A. thaliana* (WS ecotype) (Dumez *et al.*, 2006) was
169 transformed by the floral dip method using *A. tumefaciens* strain GV3101 (Clough *et al.*,
170 1998, Jyothishwaran *et al.*, 2007) according to (Facon *et al.*, 2013). Transformed plants
171 were selected for their resistance to hygromycin B. T1 seeds were sterilized according to
172 (Harrison *et al.*, 2006) and sown on petri dishes containing 1% (w/v) Murashige and Skoog
173 medium, 1% (w/v) agar and 20 $\mu g.mL^{-1}$ of hygromycin B (Sigma-Aldrich). Plates were
174 incubated in growth cabinet for 2-3 weeks at 22°C, 80% humidity and a specific
175 photoperiod according to (Harrison *et al.*, 2006). 98 hygromycin-resistant individuals were
176 transferred to soil and cultivated in a greenhouse under a 16-h light : 8-h dark photoperiod
177 (20°C during the day and 18°C at night; 100-150 $\mu E.m^{-2}.s^{-1}$ irradiance). The presence of the
178 transgene was confirmed by PCR amplification of the *glgB* sequence (glgB-For and glgB-
179 Rev primers) in 22 plants displaying a leaf iodine-staining phenotype (see below) different
180 to that of the *be2 be3* mother plant. A representative panel of eleven plants with different
181 leaf iodine-staining phenotypes was selected and T2 seeds were collected. T2 plants were
182 selected on solid MS medium as described above and 5 homozygous lines were identified by
183 segregation analysis of the hygromycin-resistance trait.
184
185 *Leaf iodine staining*
186 Plants were grown in a greenhouse under a 16-h light : 8-h dark photoperiod (20°C
187 during the day and 18°C at night; 100-150 $\mu E.m^{-2}.s^{-1}$ irradiance). Approximately 2-week-
188 old plants were harvested at the end of the day and immediately immersed in 70% hot
189 ethanol. Samples were incubated under shaking at 70°C and ethanol was replaced several
190 times until complete loss of pigments, prior to be rinsed with water and stained by a KI 1%
191 (w/v) - $I_2$ 0.1% (w/v) solution.
192
193 *Extraction and quantification of polyglucans*
194 Leaves were harvested at the end of the day, immediately frozen in liquid nitrogen

195 and stored at - 80°C until use. Two different protocols were then applied for polyglucan
196 extraction.
197 Isolation of insoluble polyglucans (for microscopy and crystallographic analysis) was
198 adapted from (Streb *et al.*, 2008). Several tens of grams of leaves were homogenized in a
199 buffered medium (0.1 M Na-acetate (pH 4.8); 0.05% Triton X-100, 2 mM EDTA) with a
200 blender, and then filtered on two layers of Miracloth (Calbiochem). SDS was added to the
201 filtrate at a final concentration of 1.5% (w/v) and the insoluble polyglucans were collected
202 by centrifugation (20 min at 20,000 g). Then, the samples were washed 4 times with water
203 and were sequentially filtered on nylon meshes of decreasing pore size, in the order: 100,
204 31 and 11 µm. The filtrates were centrifuged (10 min at 16,000 g) and the polyglucan pellet
205 was resuspended in 20% ethanol and stored at 4°C until use.
206 Extraction of insoluble and soluble polyglucans (for quantification and ultrastructure
207 analysis) was performed on 1 g of leaves using the perchloric acid method described in
208 detail in (Streb *et al.*, 2008).
209 The polyglucan content was measured by a spectrophotometric method (Enzytec™,
210 R-BIOPHARM®) following the manufacturer's instructions.
211
212 *Analysis of the ultrastructure of polyglucans*
213 The chain length distribution (CLD) of the polyglucans was determined with 200 µg
214 of purified material debranched with a mix of 4 U isoamylase (*Pseudomonas sp.*,
215 Megazyme) and 2U pullulanase (*Klebsiella planticola*, Megazyme) in sodium acetate
216 buffer (55 mM final concentration, pH3.5) incubated overnight at 42°C in a final volume of
217 500 µL. After 10 min at 100°C, the mix was desalted on Alltech™ Extract-Clean™
218 Carbograph columns (Fisher Scientific). First, columns were equilibrated with 5 mL of
219 25% acetonitrile and washed with 5 mL of deionized sterile water. Then, samples were
220 loaded on the columns and subsequently rinsed with 5ml of deionized water. Sample
221 elution was performed with 2 mL of 25% acetonitrile. The samples were lyophilized and
222 resuspended in 250 µL of deionized water. The chain length distribution of each sample
223 was determined by HPAEC-PAD analysis (Dionex® – PA200 CarboPac column) as fully
224 described in (Roussel *et al.*, 2013).

225

226 *Starch fractionation*

227 Starch fractionation (separation of high and low mass polymers) was performed by
228 size exclusion chromatography on a Sepharose CL-2B matrix. 1.2 mg of starch was
229 dispersed in 200 µL of DMSO (100%) during 15 min at 100 °C. The polymers were
230 precipitated by the addition of 800µL of absolute ethanol and left for 2h on ice. After
231 centrifugation for 5 min at 10,000 g, the pellet was solubilized in 500 µL of 10 mM NaOH
232 and loaded onto the column previously equilibrated with 10 mM NaOH (0.5 cm i.d. × 65
233 cm) at a flow rate of 12 $mL.h^{-1}$. Fractions of 300 µL were collected and the glucans were
234 detected using $I_2$ / KI solution (0.1% and 1% w/v respectively).

235

236 *Protein extraction*

237 Protein extracts were obtained from approximately 1 g of fresh leaves harvested at the
238 middle of the day and directly frozen in liquid nitrogen. Frozen leaves were finely
239 powdered and immersed in ice-cold 100 mM Tricine/KOH (pH 7.8) 5 mM $MgCl_2$, 1 mM
240 DTT containing 0.1 % (v/v) of protease inhibitor cocktail (ProteaseArrest™, G
241 Biosciences). Samples were centrifuged at 16,000 g at 4°C during 10 min. The supernatant
242 was collected and the protein content was determined by Bradford assay.

243

244 *Zymogram of branching enzyme activity*

245 Zymograms of branching enzyme activity were obtained according to the method
246 described by (Tetlow *et al.*, 2004, Tetlow *et al.*, 2008). Branching enzyme activity is
247 detected indirectly by the stimulation of phosphorylase « a ». In the presence of a high
248 concentration of Glc-1-P and the absence of Pi, phosphorylase « a » synthesizes linear
249 α(1→4)-linked polyglucans that can be branched in α(1→6) if a branching enzyme is in the
250 vicinity. Branching increases the number of available non-reducing ends and thus
251 stimulates phosphorylase « a » polymerizing activity. This leads to the synthesis of
252 branched polyglucans that can be detected in the form of dark brown bands in the gel after
253 iodine staining. In brief, 5% (w/v) polyacrylamide resolving gel in 375 mM of Tris-HCl
254 pH8.8 (non-denaturing conditions) was prepared with 3 $U.mL^{-1}$ of rabbit phosphorylase

255 « a » (Sigma), 1 mM of maltoheptaose (Sigma) and 1.5 mM of acarbose (Sigma-Aldrich)
256 and was maintained at 4°C. 60 µg of proteins were mixed with a loading solution in a 20:1
257 ratio (loading solution: 2 $mg.mL^{-1}$ of bromophenol blue and 50% (v/v) glycerol) and loaded
258 onto the gel. After migration (1 h 30 min at 15 $V.cm^{-1}$, at 4°C in 25 mM Tris / 192mM
259 Glycine buffer pH8.5), the gel was washed twice in buffer 20 mM MES and 100 mM
260 sodium citrate at pH6.6 at room temperature. After incubation for 2 h at 30°C in 20 mM
261 MES and 100 mM sodium citrate buffer (pH6.6) supplemented with 50 mM of glucose-1-
262 phosphate, 2.5 mM AMP, 1 mM EDTA, and 1 mM DTT, the gel was gently rinsed three
263 times with water and subsequently revealed with $I_2$/KI solution (0.1% / 1% (w/v).
264
265 In vitro *assay of branching enzyme activity*
266 The branching enzyme activity in leaf extracts was determined according to the
267 method described in details by (Tetlow *et al.*, 2008).
268
269 *Immunoblotting*
270 Two types of immunoblotting experiments were carried out during this work. The
271 first was performed after 100 µg of total proteins from a cell extract were separated by
272 SDS-PAGE (7.5% acrylamide and 0.1% (w/v) SDS). After migration, proteins were
273 transferred to a nitrocellulose membrane (Whatmann) with a transfer buffer (0.025 M Tris;
274 0.192 M glycine; 20% (v/v) methanol). After transfer the membrane was incubated in a
275 blocking solution (0.01 M Tris; 0.25 M NaCl; 1.5% (w/v) BSA) during 15 min and then
276 incubated overnight with the primary antibody diluted at 1/5000 in the blocking solution at
277 room temperature. Then the membrane was washed three times in TTBS (0.1 M Tris; 0.25
278 M NaCl; 0.1% (v/v) Tween 20). The membrane was incubated for 2 h with a 1/30000
279 dilution of the secondary antibody (anti-rabbit IgG- alkaline phosphatase; Sigma) at room
280 temperature. The membrane was finally rinsed three times with TTBS buffer and developed
281 with the BCIP/NTB substrate kit following manufacturer's instructions (Invitrogen).

282 In the second type of immunoblotting experiment protein extracts were treated as for BE
283 zymogram analysis described above. However, after migration, proteins were transferred to

284 a nitrocellulose membrane (Whatmann) following the protocol described above.

285 The primary antibody raised against GlgB was produced in rabbit by the inoculation
286 of a peptide specific of the *E. coli* branching enzyme (Eurogentec). Peptide sequence: $NH_2$-
287 NLYEHSDPREGYHQDW -$CONH_2$ (position 355-370 of *E. coli* GlgB protein); Protein
288 carrier: KLH.

289

290 *Transmission and scanning electron microscopy*

291 Strips of freshly cut leaves harvested at the end of the day were fixed with
292 glutaraldehyde, post-fixed with osmium tetroxide and embedded in Epon resin. 70 nm-thin
293 sections were cut with a diamond knife in a Leica UC6 microtome and post-stained with
294 periodic acid thiosemicarbazide silver proteinate (PATAg) (Gallant *et al.*, 1969). Drops of
295 dilute suspensions of purified glucans were deposited on glow-discharged carbon-coated
296 copper grids and the preparations were negatively stained with 2% uranyl acetate. All
297 specimens were observed with a Philips CM200 transmission electron microscope (TEM)
298 operating at 80 kV. Images were recorded on Kodak SO163 films. In addition, drops of
299 briefly sonicated suspensions of purified glucans were allowed to dry on freshly cleaved
300 mica and coated with Au/Pd. Secondary electron images of the specimens were recorded
301 with a FEI Quanta 250 scanning electron microscope (SEM) equipped with a field emission
302 gun and operating at 2 kV.

303

304 *Wide-angle X-ray scattering*

305 The crystallinity index of the polyglucan samples was measured by wide-angle X-ray
306 scattering following a method described by (Wattebled *et al.*, 2008).

307

308 **RESULTS**

309

310 ***Selection of Arabidopsis lines expressing GlgB***

311 *glgB* from *E. coli* was fused downstream of the nucleotide sequence encoding AtBE2
312 (At5g03650) chloroplast transit peptide. The resulting cDNA was then cloned into
313 pMDC32, a binary vector designed for transgene expression under the control of the CaMV

314 35S promoter. *be2 be3* double mutants were transformed by the floral dip method (Clough
315 *et al.*, 1998) with an *Agrobacterium tumefaciens* strain carrying the construct. Among 6000
316 plants tested, 98 transformants (T1), displaying hygromycin resistance, were selected on
317 MS agar plates. 5 independent homozygous lines were selected among their progeny (T2
318 plants) and further analyzed for their leaf iodine-staining phenotype (Figure 1). At the end
319 of the daytime period, while wild-type (WT) leaves stain black due to normal amounts of
320 starch, *be2 be3* leaves stain yellow because they lack polysaccharides. By contrast,
321 *isa1 isa3 pu1* leaves stain orange because they accumulate high amounts of phytoglycogen
322 (Wattebled *et al.*, 2008). The phenotypes of the transformants, called "β lines", were
323 intermediate between those of WT and *isa1 isa3 pu1* lines, suggesting that the
324 polysaccharide synthesis was at least partially restored. However, while β20 and β6 lines
325 stain brown, β12 stains dark brown and β1 stains dark grey, suggesting different levels of
326 complementation. β5 is noteworthy since iodine staining is not homogeneous in that line. A
327 grey stain was observed at the apex of some leaves, while other leaves remained yellow. It
328 suggests a non-homogeneous expression of the transgene in that line. For clarity, only β1,
329 β12, and β20 lines, that are representative of each phenotype, will be further presented here.
330 Results obtained for lines β5 and β6 are available as Supporting figures (Figure S7 and
331 Figure S8).
332 The *be2 be3* double mutant displays strong growth retardation probably due to the
333 over-accumulation of maltose (Dumez *et al.*, 2006). Therefore, we analyzed the
334 developmental phenotype of the transformants as well as *be2 be3* and wild-type plants
335 (Figure S2). Contrary to *be2 be3* mutant plants, GlgB-expressing lines were similar to the
336 wild type at maturity.
337
338 ***Expression and activity of GlgB***
339 The expression of GlgB in the "β" lines was confirmed by western blot using a
340 peptide-specific anti-*E. coli* BE antibody raised against a 16-mer peptide of the protein
341 (Figure 2A). As expected, while GlgB is absent in *be2 be3* and WT, a unique band of
342 approximately 85 kDa was observed in the transgenic lines. Interestingly, each of these
343 lines displays increasing band intensity in the order: β1, β12 and β20. Zymograms of BE

344 activity were obtained using cell extracts prepared from leaves harvested at the middle of
345 the light period (Figure 2B). As already described (Dumez *et al.*, 2006), no BE activity is
346 observed in the *be2 be3* mutant of Arabidopsis while WT displays one band of activity on
347 the zymogram (Figure 2B). In contrast, a large activity band of lower mobility was found in
348 the *E. coli* extract. BE electrophoretic profiles of the transgenic lines differ between each
349 other as well as from those of *E. coli* and Arabidopsis. Indeed, one band of intermediate
350 mobility (Figure 2B, a + b) is present in all extracts of the three "β" lines except in line β5
351 in which expression of GlgB seems extremely low and heterogenous throughout the plant
352 (Figure 2B). Moreover, an additional band with a higher mobility than that of Arabidopsis
353 BE is visible in line β20 (Figure 2B, c). Band intensities also vary among "β" lines, being
354 far greater in β12 and β20 extracts compared to β1 (Figure 2B).

355 Correlations between zymogram activities and *glgB* expression in the transgenic lines
356 were sought by western blot. Leaf or cell protein extracts were separated by polyacrylamide
357 gel electrophoresis in non-denaturing conditions similar to those used in the zymogram
358 assay. As expected, no cross-reaction could be seen in *Arabidopsis* WT and *be2 be3*
359 samples. One band was observed in the *E. coli* extract, the mobility of which corresponded
360 to the activity detected on the zymogram (Figure 2B and 2C). Similarly, two bands
361 corresponding to the activities observed on the zymogram were visible in the β1, β12, and
362 β20 transgenic lines (Figure 2C, a and b). However, the intensity of the two bands in line
363 β1 was lower than that of the two other transgenic lines. A third band of higher mobility
364 was also clearly visible in line β20 (Figure 2C, c) and may correspond to the high mobility
365 activity observed on the zymogram.

366 Zymogram and immunoblotting assays suggest that different levels of BE activity can
367 be found in the lines tested in this work. Thus, BE activity was measured *in vitro* by the
368 phosphorylase « a » stimulating assay using $^{14}$C-labeled Glc-1-P (Figure 2D). Leaf extracts
369 were incubated for 10, 20 or 40 min at 30°C and Glc-1-P consumption was plotted against
370 the incubation time (Figure 2D). This assay confirmed that BE activity increased in the "β"
371 lines, in the order: β1, β12 and β20. An extremely low level of activity was detected in the
372 *be2 be3* mutant of Arabidopsis (phosphorylase « a » activity is not stimulated because of
373 the lack of BE activity in this line) while WT shows significant incorporation of Glc into

374 polyglucan after 40 min of incubation.

375

376 ***Polyglucan accumulation in the glgB expressing lines***

377 Iodine-staining phenotypes of the transgenic lines expressing *glgB* suggest that starch
378 and/or water-soluble polysaccharide synthesis is at least partially restored despite the lack
379 of endogenous branching enzymes. These polyglucans were assayed after extraction from
380 leaves harvested at the end of the 16-h light period (Figure 3). Wild-type Arabidopsis plants
381 accumulate insoluble polysaccharides and only tiny amounts of non-methanol-precipitable
382 sugars (i.e. glucose and maltooligosaccharides), while methanol-precipitable
383 polysaccharides could not be detected (Figure 3). Interestingly, line β1 displayed the
384 highest amount of insoluble polyglucans among transgenic lines while it also showed the
385 lowest BE activity (Figure 2 and Figure 3). In line with this, insoluble polysaccharide
386 contents were lower in both β12 and β20, in contrast to the levels of BE activity observed
387 in these plants. Interestingly, methanol-precipitable glucans were detected at significant
388 levels in β12 and β20 compared to β1. Non-methanol-precipitable glucans were found at a
389 relatively high level in β20 (about 1 $mg.g^{-1}$ of fresh leaves) compared to the other lines
390 (0.35 $mg.g^{-1}$ in β12; 0.2 $mg.g^{-1}$ in β1; 0.05 $mg.g^{-1}$ in WT). In the same culture conditions
391 (16 h light), the *be2 be3* double mutant accumulated very high amounts of maltose (up to
392 20 $mg.g^{-1}$ of fresh weight) (Dumez *et al.*, 2006). Finally, note that the glucans accumulated
393 in the different lines analyzed in this work were degraded in the night as shown by leaves
394 iodine staining (Figure S3).

395

396 ***Observation of polyglucans accumulation in leaf chloroplasts***

397 The accumulation of polyglucans was directly observed *in planta* by transmission
398 electron microscopy (TEM - Figure 4). Ultrathin sections of leaves were observed after
399 positive staining of the polyglucans with PATAg. Flat and smooth starch granules of
400 approximately 1-3 µm were observed in WT (Figure 4A), as already described in the
401 literature. By contrast, no starch granules were detected in the *be2 be3* double mutant, in
402 agreement with the phenotype already described for this line (Figure 4B) (Dumez *et al.*,
403 2006). The *isa1 isa3 pu1* triple mutant was included in this analysis as a starchless

404 phytoglycogen-accumulating line. Phytoglycogen was visible in the form of very small and
405 polydisperse particles homogeneously distributed in the stroma of the chloroplasts (Figure
406 4C). Different types of particles were observed in the three lines expressing *glgB*. Lines β1
407 and β12 accumulated 0.2 - 3 µm-large and irregularly shaped particles (Figure 4D and 4E,
408 respectively), while β20 contained significantly smaller and highly polydisperse particles
409 (Figure 4F). The larger objects could reach 1 µm in size but most particles were smaller
410 than 0.2 µm. The image of β20 is thus similar to that of *isa1 isa3 pu1* (Figure 4C) although
411 no large aggregates were observed in the images of the triple DBE mutant. The surface of
412 the particles was irregular and rather rough in β1 while it was smoother in β12. In both
413 specimens, the fact that the larger particles may correspond to the aggregation of smaller
414 units cannot be excluded.
415
416 ***Morphology of purified insoluble and soluble polyglucans***
417 The insoluble polyglucans were observed by scanning electron microscopy (SEM)
418 after extraction from leaves and purification (Figure 5). In WT, starch granules appeared as
419 polygonal flat particles with a smooth surface, as usually observed for Arabidopsis starch
420 granules (Figure 5A). Their size typically ranged between 2 and 5 µm. The identification of
421 individual particles in extracts from the transgenic lines was rather difficult as the images
422 showed that the particles were highly polydisperse and with very irregular shapes (Figure
423 5B-5D). Artefactual particle aggregation could not be excluded since, during purification,
424 the fraction were extensively washed using repeated centrifugation. Local concentration of
425 the smallest particles upon drying on the supporting mica was also unavoidable as they
426 were more easily subject to the capillary effects of evaporating water. Nevertheless, the
427 images were in fairly good agreement with what was expected from the TEM observation
428 of ultrathin sections of leaves (Figure 4D-4F), with the particle average size clearly
429 decreasing with increasing GlgB activity. In particular, the particles in β1 exhibited
430 tortuous shapes and a rather rough surface (Figure 5B), while two polyglucan populations
431 were observed in β20 (Figure 5D): one with an average size ranging from 500 nm to 1 µm,
432 quite similar to those observed in β12 (Figure 5C), and one containing smaller particles
433 (< 200 nm) whose morphology was hardly resolved by SEM (inset Figure 5D).

434 Higher resolution images of the insoluble polyglucans were recorded by TEM of
435 negatively stained preparations. As the particles extracted from β1 were too large to be
436 observed with this technique, only particles extracted from β12 and β20 are shown in
437 Figure 6. Moreover, only the smallest of these insoluble particles could be properly stained
438 and observed with sufficient detail. Consequently, the images illustrate the morphology of
439 this fraction of particles but may not represent that of the larger objects.

440 The insoluble polyglucans in β12 often appeared as aggregates of smaller particles
441 with various shapes and sizes (Figure 6A and 6B). 200 nm bulky and rather smooth
442 spheroidal particles could be recognized, often in contact with multilobular less well-
443 defined material. The particles in β20 are more flat and exhibit a clear multilobular aspect
444 (Figure 6C and 6D). Their average size is still around a few hundreds nanometers but they
445 seem to be composed of 50-70 nm subunits. Although it is difficult to see if the larger
446 particles are aggregates of individual subunits formed upon centrifugation and/or drying,
447 the morphology resembles that of the so-called α-particles observed in liver glycogen and
448 constituted of smaller β-subunits (Ryu *et al.*, 2009, Sullivan *et al.*, 2012).

449 TEM images of the polyglucans isolated from the soluble fractions from β12 and β20
450 are shown in Figure 7. In both cases, 20-30 nm particles are observed (Figure 7A and 7B)
451 whose aspect and size distribution are very similar to those of maize phytoglycogen (Figure
452 7C).

453

454 ***Ultrastructure of insoluble and soluble polyglucans***

455 The ultrastructure of insoluble and soluble polyglucans was determined and compared
456 to that of reference samples. First, insoluble polyglucans were fractionated by size
457 exclusion chromatography on Sepharose CL-2B® (Figure 8). WT starch shows a regular
458 elution profile exhibiting two peaks (Figure 8A). The first peak corresponds to high-mass
459 amylopectin (between 10 and 13 mL) while the second broader peak corresponds to the
460 low-mass amylose (between 16 and 27 mL). The elution profile of insoluble polyglucans
461 for line β1 also contains two distinct peaks corresponding to high-mass (same elution
462 volume as WT amylopectin) and low-mass material (elution volume equivalent to that of
463 WT amylose), respectively (Figure 8B). However, the peak of low-mass material is much

464 higher and slightly shifted towards lower masses (to the right on the diagram) compared to
465 WT amylose. Moreover, the $\lambda_{max}$ of the iodine-polysaccharide complex for high-mass
466 material in line β1 is 10 nm higher compared to that of WT amylopectin. This suggests that
467 this material is composed, on average, of longer-chain glucans than WT amylopectin. β12
468 and β20 insoluble polyglucans display more or less the same elution profile (Figure 8C and
469 8D, respectively). A unique large peak of high-mass material is observed, the elution
470 profile of which is equivalent to that of WT amylopectin. Contrary to WT and β1 insoluble
471 polyglucans, no distinct peak of low-mass material was seen in β12 and β20 lines. In
472 addition, the $\lambda_{max}$ of the high-mass material in these two lines was decreased by 10 nm
473 compared to WT amylopectin, suggesting that the length of the glucans is shorter on
474 average (Table1).

475 The crystallinity index of the insoluble polyglucans was determined by wide-angle X-
476 ray scattering. The analyses were performed on two samples of polyglucans extracted from
477 two plant preparations cultivated independently (Table 1). All samples are of B-type
478 allomorph. The WT starch granules have a crystallinity index of 33%, in agreement with
479 previous reports on Arabidopsis starch (Wattebled *et al.*, 2008). The β1 and β12 insoluble
480 polyglucans display a lower crystallinity index (27 and 20%, respectively), while the β20
481 insoluble glucans have the lowest crystallinity index (13%) among those analyzed in this
482 work.

483 The chain length distribution (CLD) profile of the insoluble polyglucans was
484 established after debranching with a mixture of bacterial isoamylase and pullulanase. The
485 resulting linear glucans were separated and quantified by HPAEC-PAD (Figure 9). The
486 profile of β1 polyglucans has a DP max of 12-13 glucosyl residues identical to WT starch
487 (Figure 9A and 9C). However, the fraction of DP 5-18 glucans is higher and the fraction of
488 DP 21-40 is lower in β1 compared to WT. The higher fraction of short glucans (DP<13)
489 that do not interact with iodine may explain the increase of the $\lambda_{max}$ of the iodine-
490 polyglucan complex observed in this sample (Table 1). The β12 insoluble polyglucan has a
491 profile similar to that of β1 although the fraction of DP 5-11 glucans is higher, especially at
492 DP 6-7 (Figure 9A). In β20, the $DP_{max}$ is at DP 7 and the profile strongly resembles that of
493 the insoluble glucan synthesized by the *Arabidopsis isa1 isa3 pu1* triple mutant (Figure 9B)

494 apart from for a strong depletion of DP 3-4 glucans in β20 that is probably due to the
495 presence of DBE activity in that line compared to the triple DBE mutant.

496 The branching degree of the insoluble polyglucans was estimated according to the
497 method described in (Szydlowski *et al.*, 2011) (Table 1). WT, β1, β12 and β20 polyglucans
498 had branching degrees of 5.1, 6.1, 6.8 and 7.3%, respectively. The branching degree of the
499 phytoglycogen of the *Arabidopsis isa1 isa3 pu1* triple mutant was estimated at 8.1%, a
500 value very close to that previously reported (Szydlowski *et al.*, 2011).

501 The CLD profiles were also established for the soluble polyglucans isolated from the
502 transgenic lines. The corresponding profiles were compared to that of rabbit liver glycogen
503 (Figure S4). In all cases, DP 7 chains were the most abundant among those analyzed.
504 Although the profiles of the transgenic lines were all similar, they were different to that of
505 glycogen with a significant excess of DP 5-13 chains and a deficit in DP > 17 chains.

506

507 **DISCUSSION**

508 The suppression of both BE2 and BE3 in *Arabidopsis* resulted in the complete loss
509 of starch branching enzyme activity (Figure 2B and 2D) and the loss of starch synthesis and
510 was accompanied by the accumulation of maltose and plant growth retardation (Dumez *et*
511 *al.*, 2006). Other starch metabolizing enzymes were not affected by the mutations. Thus, the
512 *be2 be3* double mutant represents an excellent model to investigate the ability of GlgB to
513 restore starch or starch-like polyglucan synthesis in Arabidopsis.

514 The expression of *glgB* in *A. thaliana* was successfully achieved after
515 transformation of the corresponding cDNA into *be2 be3* plants. The corresponding protein
516 was detected by immunoblot analysis of leaf extracts of several independently transformed
517 plants (Figures 2A and 2C) and the branching activity of the enzyme was also detected
518 (Figures 2B and 2D). Different levels of expression were obtained, although all plants
519 analyzed in this study were homozygous for the transgene. Indeed, the level of BE activity
520 was much higher in β20 compared to β12, and most notably compared to β1 which had the
521 lowest BE activity as measured by zymogram and *in vitro* radioactive assay (Figures 2B
522 and 2D). These levels of activity were correlated with GlgB protein contents. Immunoblot

523 analysis performed under denaturing or non-denaturing conditions (Figures 2A and 2C
524 respectively) showed that the content of GlgB is higher in β20 than in β12 and even more
525 than in β1, which is in good agreement with the level of activity assayed in each line.
526 Interestingly, immunoblot analysis performed under non-denaturing conditions (Figure 2C)
527 revealed several bands reacting with the anti-GlgB antibody in the transgenic lines. Two
528 major bands (Figure 2B bands a and b) were detected in all three lines and a third band
529 (Figure 2B band c) of higher mobility but lower intensity was specifically observed in β20.
530 Two additional lines were analyzed during this work: β5 and β6. Corresponding results are
531 presented as Supporting data in the form of Figures S6, S7 and S8 and confirm the results
532 presented above. Line β5, which has a very low GlgB activity, displays a phenotype similar
533 to that of β1. Conversely line β6, that has high GlgB activity, is similar to β20. This result
534 suggests that GlgB is either post-translationally modified when expressed in *Arabidopsis* or
535 is involved in the formation of protein complexes (homo or heteromeric complexes) with
536 different electrophoretic mobility (Tetlow *et al.*, 2004, Makhmoudova *et al.*, 2014).

537 Although GlgB was expressed and active in all transgenic lines, the phenotype of
538 polyglucan accumulation was different from one line to another. Indeed, albeit displaying
539 the lowest GlgB expression level, β1 accumulated polyglucans with a structure close to that
540 of WT starch. These polyglucans had a granular morphology and individual particles were
541 observed in the stroma of the chloroplast (Figure 4). These granules had a size similar to
542 that of WT starch although their surface appeared to be rougher. Smaller PATAg-stained
543 particles, with a size well below 1 µm, were also dispersed throughout the stroma of β1
544 chloroplasts. Moreover, the β1 insoluble polyglucan fraction was partially crystalline (27%
545 compared to 33% for WT starch) and was composed of both high-mass amylopectin-like
546 material and low-mass amylose-like material (Figure 8). Further, the CLD profile after
547 debranching was similar to that of WT starch although it was enriched in DP 5-19 chains
548 (with a $DP_{max}$ at 12 glucose residues such as in WT starch) and depleted in DP 21-40 chains
549 (Figure 9). As a whole, the β1 polyglucan can be considered as starch-like implying that a
550 bacterial glycogen BE can sustain the synthesis of such specifically ordered polysaccharide
551 when expressed in plants. It follows that the final distribution of the branch points within

552 starch and consequently the properties of the synthesized polyglucan (crystallinity, water-
553 insolubility, granular morphology, amylopectin $DP_{max}$ at 12-13, and the presence of
554 amylose) is not solely under the control of starch branching enzymes (although branching
555 enzyme activity is mandatory to create α(1→6) linkages). Otherwise, expression of a
556 bacterial glycogen-branching enzyme in the plant would have resulted in the synthesis of
557 soluble and amorphous glycogen-like polymers. Nevertheless, the polyglucan that
558 accumulates in β1 can not be regarded as true WT starch and several hypotheses can be
559 proposed which could explain why this is the case. Firstly, GlgB is expressed in
560 *Arabidopsis* under the control of the constitutive 35S promoter. Consequently, GlgB is
561 likely expressed linearly during the day and the night, which may influence the final
562 structure of the synthesized polyglucan. However, the expression profiles of the
563 endogenous BEs (BE2 and BE3) are not similar during the day/night cycle (Smith *et al.*,
564 2004) although their functions are largely overlapping (Dumez *et al.*, 2006). Indeed, BE2
565 exhibits only slightly higher expression in the day compared to the night. BE3, expression
566 is significantly higher during the day compared to night and displays an expression pattern
567 that resembles that of enzymes involved in starch degradation (Smith *et al.*, 2004),
568 although, more recently, BE3 protein abundance was reported as unmodified throughout
569 the day/night cycle (Skeffington *et al.*, 2014). The second hypothesis relies to the intrinsic
570 properties of GlgB activity. Indeed, starch BE isoforms have different catalytic properties
571 (Tetlow, 2012). In *A. thaliana*, in contrast to other plants and to other dicots, only class-II
572 branching enzymes (BE2 and BE3) have been described so far. However, because of its
573 catalytic properties, GlgB can be classified in the class-I plant branching enzymes and
574 preferentially transfers DP 6-15 chains (with a maximum for DP 10-12 chains) (Guan *et al.*,
575 1997, Sawada *et al.*, 2014). Therefore it is not surprising that the expression of a class-I BE
576 instead of class-II BEs results in modifications in the structure of the synthesized
577 polysaccharide compared to the wild type. Another explanation relates to enzyme complex
578 formation. It is now well established that some of the starch metabolizing enzymes interact
579 to form hetero-multimeric complexes (Hennen-Bierwagen *et al.*, 2008, Tetlow *et al.*, 2008,
580 Hennen-Bierwagen *et al.*, 2009). Branching enzymes are important components of these
581 complexes as shown in the endosperm of cereals (Liu *et al.*, 2009, Liu *et al.*, 2012a, Liu *et*

582 *al.*, 2012b). Although it has not been shown yet, it is likely that starch-metabolizing
583 enzymes also organize in the form of multisubunit complexes in Arabidopsis. It is highly
584 probable that BE2/BE3 and GlgB are engaged in different protein complexes or simply that
585 GlgB is unable to interact with other endogenous plant enzymes. This could result in the
586 modification of other starch-metabolizing activities and consequently polyglucan structure.
587 Even if enzymes of starch synthesis do not physically interact in Arabidopsis chloroplasts,
588 their activities must still be interdependent in order to produce the final structure of
589 amylopectin. Removing one or several enzymes of the pathway could alter the activity of
590 others whose normal activity depends on the presence of the complete set of enzymes
591 (Szydlowski *et al.*, 2011, Nakamura *et al.*, 2012, Abe *et al.*, 2014, Brust *et al.*, 2014,
592 Nakamura *et al.*, 2014). GlgB may only partially counterbalance the lack of both BE2 and
593 BE3 in the transgenic lines, which, in turn, may alter other starch-metabolizing activities.
594 Lastly, some starch-metabolizing enzymes are regulated by the redox state of the cell or the
595 organelle where the pathway occurs (Glaring *et al.*, 2012, Lepisto *et al.*, 2013). It is
596 possible that GlgB does not behave like Arabidopsis BEs which are redox sensitive
597 (Glaring *et al.*, 2012), thus modifying the branching activity in the transgenic lines and
598 explaining why it is not possible to restore a true WT phenotype.

599 Finally, it should be emphasized that the ability to form starch-like structures
600 depends on the level of branching enzyme activity of GlgB. Indeed, β20, which possessed
601 the highest GlgB activity, synthesizes polyglucans whose structure resembles more or less
602 that of the residual insoluble glucans isolated from Arabidopsis DBE mutants (Wattebled *et*
603 *al.*, 2008). The β12 line, that had a GlgB activity intermediate between that of β1 and β20,
604 displays an intermediate polyglucan-accumulating phenotype. Debranching enzyme activity
605 level was estimated in the different lines by zymogram analysis (Figure S5). No obvious
606 modification of isoamylase activity was detected in the GlgB-expressing plants compared
607 to the wild type. Starch synthase activity was also evaluated with zymograms (Figure S6).
608 SS1 and SS3 are the two major isoforms of starch synthases encompassing over 90% of the
609 elongating activity measured in *Arabidopsis* leaf extracts (Szydlowski *et al.*, 2011). Starch
610 synthase activities were unmodified in the *be2 be3* mutant (Dumez *et al.*, 2006). Both SS1

611 and SS3 activities were reduced in β1 compared to WT. The activity of SS1 was slightly
612 higher in β12 and β20 compared to WT whereas SS3 was, to some extent, reduced. At this
613 stage it is unclear why starch synthase activity is modified in the transgenic lines, especially
614 in β1. Nevertheless, despite possessing the lowest starch synthase activity, β1 is the GlgB
615 expressing line accumulating the highest amount of insoluble polyglucans. Thus the
616 remaining SS activity in β1 appears in be in excess of that needed to allow the synthesis of
617 the insoluble polyglucan, and does not seem to be a limiting factor.

618 Thus, in a context of non-limiting starch synthase activity, the accumulation of the
619 insoluble and soluble polyglucans in β20 occurs under circumstances of over-branching
620 which cannot be balanced by the debranching activity of endogenous isoamylases and
621 pullulanase. This results in a higher branching degree (7.3%) and a very low crystallinity
622 index (13%) of the insoluble polyglucans in β20. Such increase of the branching degree of
623 the polyglucan produced in plants after the expression of *E. coli* GlgB has already been
624 described in potato and rice (Kortstee *et al.*, 1996, Kim *et al.*, 2005). In both cases, the
625 number of branch points of amylopectin was significantly increased. However, because
626 endogenous BE activity was not knocked down in these plants the actual contribution of
627 GlgB for the synthesis of the highly branched starch was impossible to determine.

628 Our result suggests that a finely tuned balance between branching and debranching
629 activities is probably acting *in planta* to control α(1→6) linkage placement and number,
630 and consequently to allow the formation of starch or starch-like polyglucan. Figure 10 is an
631 attempt to model our interpretation of the results generated in this work. As a model, it is
632 likely a simplified view of reality (for instance starch synthases are not included in the
633 model) and was conceptualized from the results of the expression of a bacterial enzyme in
634 plants. However, we suggest that it could be generalized to any situation where the balance
635 between BE and DBE activity is compromised. For instance, in rice, the endogenous BEIIb
636 isoform was expressed in a BEIIb-defective mutant by expression of the corresponding
637 structural gene (Tanaka *et al.*, 2004). Overexpression of the protein and of the
638 corresponding activity was obtained in one of the transgenic lines leading to the
639 accumulation of significantly higher amount of soluble polyglucan compared to the wild

640 type (almost three times more). This was accompanied by enrichment in DP<15 glucans of
641 amylopectin and alteration of the crystalline structure of starch.

642 Nevertheless expression of GlgB did not restore the synthesis of true WT starch,
643 possibly because GlgB activity cannot be regulated in the same way as endogenous BEs.
644 Protein complexes and thus other enzyme activities (starch synthases for instance) might be
645 affected by the lack of endogenous BEs, leading to the synthesis of structurally modified
646 polyglucan as frequently observed in mutants defective for enzymes of the pathway.

647

648

649 **ACKNOWLEDGEMENTS**

650 The authors thank Dr. Nicolas Szydlowski for fruitful discussions and critical
651 reading of the manuscript, the NanoBio-ICMG Electron Microscopy Platform (Grenoble)
652 and gratefully acknowledge the financial support of Agence Nationale de la Recherche
653 (contract # ANR-11-BSV6-0003) and the Natural Sciences and Engineering Research
654 Council of Canada (Team Discovery Grant, number 435781, MJE, IJT).

655

656 **REFERENCES**


657 Abe N., Asai H., Yago H., Oitome N., Itoh R., Crofts N., Nakamura Y. & Fujita N. (2014)
658 Relationships between starch synthase I and branching enzyme isozymes
659 determined using double mutant rice lines. *BMC Plant Biology*, **14**, 80.
660 Ball S., Guan H.-P., James M., Myers A., Keeling P., Mouille G., Buléon A., Colonna P. &
661 Preiss J. (1996) From Glycogen to Amylopectin: A Model for the Biogenesis of the
662 Plant Starch Granule. *Cell*, **86**, 349-352.
663 Bertoft E. (2004) On the nature of categories of chains in amylopectin and their connection
664 to the super helix model. *Carbohydrate Polymers*, **57**, 211-224.
665 Bertoft E. (2013) On the building block and backbone concepts of amylopectin structure.
666 *Cereal Chemistry*, **90**, 294-311.
667 Brust H., Lehmann T., D'Hulst C. & Fettke J. (2014) Analysis of the functional interaction
668 of Arabidopsis starch synthase and branching enzyme isoforms reveals that the
669 cooperative action of SSI and BEs results in glucans with polymodal chain length
670 distribution similar to amylopectin. *PLoS One*, **9**, e102364.
671 Buleon A., Colonna P., Planchot V. & Ball S. (1998) Starch granules: structure and
672 biosynthesis. *International Journal of Biological Macromolecules*, **23**, 85-112.
673 Burton R.A., Bewley J.D., Smith A.M., Bhattacharyya M.K., Tatge H., Ring S., Bull V.,
674 Hamilton W.D. & Martin C. (1995) Starch branching enzymes belonging to distinct
675 enzyme families are differentially expressed during pea embryo development. *Plant*
676 *J*, **7**, 3-15.
677 Clough S.J. & Bent A.F. (1998) Floral dip: a simplified method for Agrobacterium-
678 mediated transformation of Arabidopsis thaliana. *Plant J*, **16**, 735-743.
679 Delatte T., Trevisan M., Parker M.L. & Zeeman S.C. (2005) Arabidopsis mutants *Atisa1*
680 and *Atisa2* have identical phenotypes and lack the same multimeric isoamylase,
681 which influences the branch point distribution of amylopectin during starch
682 synthesis. *Plant J*, **41**, 815-830.
683 Dumez S., Wattebled F., Dauvillée D., Delvallé D., Planchot V., Ball S.G. & D'Hulst C.
684 (2006) Mutants of Arabidopsis lacking starch branching enzyme II substitute

685 plastidial starch synthesis by cytoplasmic maltose accumulation. *Plant Cell*, **18**,
686 2694-2709.
687 Facon M., Lin Q., Azzaz A.M., Hennen-Bierwagen T.A., Myers A.M., Putaux J.-L.,
688 Roussel X., D'Hulst C. & Wattebled F. (2013) Distinct functional properties of
689 isoamylase-type starch debranching enzymes in monocot and dicot leaves. *Plant*
690 *Physiol*, **163**, 1363-1375.
691 Fisher D.K., Gao M., Kim K.N., Boyer C.D. & Guiltinan M.J. (1996) Two closely related
692 cDNAs encoding starch branching enzyme from Arabidopsis thaliana. *Plant Mol*
693 *Biol*, **30**, 97-108.
694 French D. (1972) Fine structure of starch and its relationship to the organization of starch
695 granules. *Journal of the Japanese Society of Starch Science*, **19**, 8-25.
696 Fujita N. & Nakamura Y. (2012) Distinct and overlapping functions of starch synthase
697 isoforms. In: *Starch: Origins, Structure and Metabolism.* (ed I.J. Tetlow), pp. 115-
698 140. Society for Experimental Biology, London, UK.
699 Gallant D. & Guilbot A. (1969) Etude de l'ultrastructure du grain d'amidon à l'aide de
700 nouvelles méthodes de préparation en microscopie électronique. *Die stärke*, **6**, 156-
701 163.
702 Glaring M.A., Skryhan K., Kotting O., Zeeman S.C. & Blennow A. (2012) Comprehensive
703 survey of redox sensitive starch metabolising enzymes in Arabidopsis thaliana.
704 *Plant Physiol Biochem*, **58**, 89-97.
705 Guan H., Kuriki T., Sivak M. & Preiss J. (1995) Maize branching enzyme catalyzes
706 synthesis of glycogen-like polysaccharide in glgB-deficient Escherichia coli. *Proc*
707 *Natl Acad Sci U S A*, **92**, 964-967.
708 Guan H., Li P., Imparl-Radosevich J., Preiss J. & Keeling P. (1997) Comparing the
709 Properties of *Escherichia coli* Branching Enzyme and Maize Branching Enzyme.
710 *Archives of Biochemistry and Biophysics*, **342**, 92-98.
711 Guan H.P., Baba T. & Preiss J. (1994) Expression of branching enzyme I of maize
712 endosperm in Escherichia coli. *Plant Physiol.*, **104**, 1449-1453.
713 Guan H.P. & Preiss J. (1993) Differentiation of the properties of the branching isozymes
714 from maize (Zea mays). *Plant Physiol*, **102**, 1269-1273.

715 Harrison S.J., Mott E.K., Parsley K., Aspinall S., Gray J.C. & Cottage A. (2006) A rapid
716 and robust method of identifying transformed Arabidopsis thaliana seedlings
717 following floral dip transformation. *Plant Methods*, **2**, 19.
718 Hennen-Bierwagen T.A., Lin Q., Grimaud F., Planchot V., Keeling P.L., James M.G. &
719 Myers A.M. (2009) Proteins from multiple metabolic pathways associate with
720 starch biosynthetic enzymes in high molecular weight complexes: a model for
721 regulation of carbon allocation in maize amyloplasts. *Plant Physiol*, **149**, 1541-
722 1559.
723 Hennen-Bierwagen T.A., Liu F., Marsh R.S., Kim S., Gan Q., Tetlow I.J., Emes M.J.,
724 James M.G. & Myers A.M. (2008) Starch biosynthetic enzymes from developing
725 maize endosperm associate in multisubunit complexes. *Plant Physiol*, **146**, 1892-
726 1908.
727 Hizukuri S. (1986) Polymodal distribution of the chain lengths of amylopectins, and its
728 significance. *Carbohydrate Research*, **147**, 342-347.
729 Huang X.-F., Nazarian-Firouzabadi F., Vincken J.-P., Ji Q., Suurs L.C.J.M., Visser R.G.F.
730 & Trindade L.M. (2013) Expression of an engineered granule-bound Escherichia
731 coli glycogen branching enzyme in potato results in severe morphological changes
732 in starch granules. *Plant Biotechnology Journal*, **11**, 470-479.
733 James M.G., Robertson D.S. & Myers A.M. (1995) Characterization of the maize gene
734 sugary1, a determinant of starch composition in kernels. *Plant Cell*, **7**, 417-429.
735 Jyothishwaran G., Kotresha D., Selvaraj T., Srideshikan S.M., Rajvanshi P.K. &
736 Jayabaskaran C. (2007) A modified freeze-thaw method for efficient transformation
737 of Agrobacterium tumefaciens. *Current Science*, **93**, 770-772.
738 Kim W.S., Kim J., Krishnan H.B. & Nahm B.H. (2005) Expression of Escherichia coli
739 branching enzyme in caryopses of transgenic rice results in amylopectin with an
740 increased degree of branching. *Planta*, **220**, 689-695.
741 Kortstee A.J., Vermeesch A.M., de Vries B.J., Jacobsen E. & Visser R.G. (1996)
742 Expression of *Escherichia coli* branching enzyme in tubers of amylose-free
743 transgenic potato leads to an increased branching degree of the amylopectin. *Plant*
744 *J*, **10**, 83-90.

745 Lepisto A., Pakula E., Toivola J., Krieger-Liszkay A., Vignols F. & Rintamaki E. (2013)
746 Deletion of chloroplast NADPH-dependent thioredoxin reductase results in inability
747 to regulate starch synthesis and causes stunted growth under short-day
748 photoperiods. *J Exp Bot*, **64**, 3843-3854.
749 Liu F., Ahmed Z., Lee E.A., Donner E., Liu Q., Ahmed R., Morell M.K., Emes M.J. &
750 Tetlow I.J. (2012a) Allelic variants of the amylose extender mutation of maize
751 demonstrate phenotypic variation in starch structure resulting from modified
752 protein-protein interactions. *J Exp Bot*, **63**, 1167-1183.
753 Liu F., Makhmoudova A., Lee E.A., Wait R., Emes M.J. & Tetlow I.J. (2009) The amylose
754 extender mutant of maize conditions novel protein-protein interactions between
755 starch biosynthetic enzymes in amyloplasts. *J Exp Bot*, **60**, 4423-4440.
756 Liu F., Romanova N., Lee E.A., Ahmed R., Evans M., Gilbert E.P., Morell M.K., Emes
757 M.J. & Tetlow I.J. (2012b) Glucan affinity of starch synthase IIa determines
758 binding of starch synthase I and starch-branching enzyme IIb to starch granules.
759 *Biochem J*, **448**, 373-387.
760 Makhmoudova A., Williams D., Brewer D., Massey S., Patterson J., Silva A., Vassall K.A.,
761 Liu F., Subedi S., Harauz G., Siu K.W., Tetlow I.J. & Emes M.J. (2014)
762 Identification of multiple phosphorylation sites on maize endosperm starch
763 branching enzyme IIb, a key enzyme in amylopectin biosynthesis. *J Biol Chem*,
764 **289**, 9233-9246.
765 Melendez-Hevia E., Waddell T.G. & Shelton E.D. (1993) Optimization of molecular design
766 in the evolution of metabolism: the glycogen molecule. *Biochem J*, **295 ( Pt 2)**, 477-
767 483.
768 Mouille G., Maddelein M.L., Libessart N., Talaga P., Decq A., Delrue B. & Ball S. (1996)
769 Preamylopectin processing: a mandatory step for starch biosynthesis in plants. *Plant*
770 *Cell*, **8**, 1353-1366.
771 Myers A.M., Morell M.K., James M.G. & Ball S.G. (2000) Recent progress toward
772 understanding biosynthesis of the amylopectin crystal. *Plant Physiol*, **122**, 989-997.
773 Nakamura Y. (1996) Some properties of starch debranching enzymes and their possible
774 role in amylopectin biosynthesis. *Plant Science*, **121**, 1-18.

775 Nakamura Y., Aihara S., Crofts N., Sawada T. & Fujita N. (2014) In vitro studies of
776 enzymatic properties of starch synthases and interactions between starch synthase I
777 and starch branching enzymes from rice. *Plant Sci*, **224**, 1-8.
778 Nakamura Y., Ono M., Utsumi C. & Steup M. (2012) Functional interaction between
779 plastidial starch phosphorylase and starch branching enzymes from rice during the
780 synthesis of branched maltodextrins. *Plant Cell Physiol*, **53**, 869-878.
781 Pfister B., Lu K.J., Eicke S., Feil R., Lunn J.E., Streb S. & Zeeman S.C. (2014) Genetic
782 evidence that chain length and branch point distributions are linked determinants of
783 starch granule formation in Arabidopsis. *Plant Physiol*, **165**, 1457-1474.
784 Rahman A., Wong K., Jane J., Myers A.M. & James M.G. (1998) Characterization of SU1
785 isoamylase, a determinant of storage starch structure in maize. *Plant Physiol*, **117**,
786 425-435.
787 Roach P.J., Depaoli-Roach A.A., Hurley T.D. & Tagliabracci V.S. (2012) Glycogen and its
788 metabolism: some new developments and old themes. *Biochem J*, **441**, 763-787.
789 Robin J.P., Mercier C., Charbonniere R. & Guilbot A. (1974) Lintnerized Starches. Gel
790 Filtration and Enzymatic Studies of Insoluble Residues from Prolonged Acid
791 Treatment of Potato Starch. *Cereal Chemistry*, **51**, 389-405.
792 Roussel X., Lancelon-Pin C., Vikso-Nielsen A., Rolland-Sabate A., Grimaud F., Potocki-
793 Veronese G., Buleon A., Putaux J-L. & D'Hulst C. (2013) Characterization of
794 substrate and product specificity of the purified recombinant glycogen branching
795 enzyme of Rhodothermus obamensis. *Biochim Biophys Acta*, **1830**, 2167-2177.
796 Ryu J.H., Drain J., Kim J.H., McGee S., Gray-Weale A., Waddington L., Parker G.J.,
797 Hargreaves M., Yoo S.H. & Stapleton D. (2009) Comparative structural analyses of
798 purified glycogen particles from rat liver, human skeletal muscle and commercial
799 preparations. *Int J Biol Macromol*, **45**, 478-482.
800 Satoh H., Nishi A., Yamashita K., Takemoto Y., Tanaka Y., Hosaka Y., Sakurai A., Fujita
801 N. & Nakamura Y. (2003) Starch-Branching Enzyme I-Deficient Mutation
802 Specifically Affects the Structure and Properties of Starch in Rice Endosperm.
803 *Plant Physiol.*, **133**, 1111-1121.

804 Sawada T., Nakamura Y., Ohdan T., Saitoh A., Francisco P.B., Jr., Suzuki E., Fujita N.,
805 Shimonaga T., Fujiwara S., Tsuzuki M., Colleoni C. & Ball S. (2014) Diversity of
806 reaction characteristics of glucan branching enzymes and the fine structure of alpha-
807 glucan from various sources. *Arch Biochem Biophys*, **562**, 9-21.
808 Schwall G.P., Safford R., Westcott R.J., Jeffcoat R., Tayal A., Shi Y.-C., Gidley M.J. &
809 Jobling S.A. (2000) Production of very-high-amylose potato starch by inhibition of
810 SBE A and B. *Nat Biotech*, **18**, 551-554.
811 Seo B.S., Kim S., Scott M.P., Singletary G.W., Wong K.S., James M.G. & Myers A.M.
812 (2002) Functional interactions between heterologously expressed starch-branching
813 enzymes of maize and the glycogen synthases of Brewer's yeast. *Plant Physiol*, **128**,
814 1189-1199.
815 Skeffington A.W., Graf A., Duxbury Z., Gruissem W. & Smith A.M. (2014) Glucan, Water
816 Dikinase Exerts Little Control over Starch Degradation in Arabidopsis Leaves at
817 Night. *Plant Physiology*, **165**, 866-879.
818 Smith S.M., Fulton D.C., Chia T., Thorneycroft D., Chapple A., Dunstan H., Hylton C.,
819 Zeeman S.C. & Smith A.M. (2004) Diurnal Changes in the Transcriptome Encoding
820 Enzymes of Starch Metabolism Provide Evidence for Both Transcriptional and
821 Posttranscriptional Regulation of Starch Metabolism in Arabidopsis Leaves. *Plant*
822 *Physiol.*, **136**, 2687-2699.
823 Streb S., Delatte T., Umhang M., Eicke S., Schorderet M., Reinhardt D. & Zeeman S.C.
824 (2008) Starch granule biosynthesis in Arabidopsis is abolished by removal of all
825 debranching enzymes but restored by the subsequent removal of an endoamylase.
826 *Plant Cell*, **20**, 3448-3466.
827 Sullivan M.A., O'Connor M.J., Umana F., Roura E., Jack K., Stapleton D.I. & Gilbert R.G.
828 (2012) Molecular insights into glycogen alpha-particle formation.
829 *Biomacromolecules*, **13**, 3805-3813.
830 Szydlowski N., Ragel P., Hennen-Bierwagen T.A., Planchot V., Myers A.M., Merida A.,
831 d'Hulst C. & Wattebled F. (2011) Integrated functions among multiple starch
832 synthases determine both amylopectin chain length and branch linkage location in
833 Arabidopsis leaf starch. *J Exp Bot*, **62**, 4547-4559.

834 Tanaka N., Fujita N., Nishi A., Satoh H., Hosaka Y., Ugaki M., Kawasaki S. & Nakamura
835 Y. (2004) The structure of starch can be manipulated by changing the expression
836 levels of starch branching enzyme IIb in rice endosperm. *Plant Biotechnology*
837 *Journal*, **2**, 507-516.
838 Tetlow I.J. (2012) Branching enzymes and their role in determining structural and
839 functional properties of polyglucans. In: *Starch: Origins, Structure and Metabolism.*
840 (ed I.J. Tetlow), pp. 141-178. Society for Experimental Biology, London, UK.
841 Tetlow I.J., Beisel K.G., Cameron S., Makhmoudova A., Liu F., Bresolin N.S., Wait R.,
842 Morell M.K. & Emes M.J. (2008) Analysis of protein complexes in wheat
843 amyloplasts reveals functional interactions among starch biosynthetic enzymes.
844 *Plant Physiol*, **146**, 1878-1891.
845 Tetlow I.J., Wait R., Lu Z., Akkasaeng R., Bowsher C.G., Esposito S., Kosar-Hashemi B.,
846 Morell M.K. & Emes M.J. (2004) Protein phosphorylation in amyloplasts regulates
847 starch branching enzyme activity and protein-protein interactions. *Plant Cell*, **16**,
848 694-708.
849 Wattebled F., Dong Y., Dumez S., Delvalle D., Planchot V., Berbezy P., Vyas D., Colonna
850 P., Chatterjee M., Ball S. & D'Hulst C. (2005) Mutants of Arabidopsis lacking a
851 chloroplastic isoamylase accumulate phytoglycogen and an abnormal form of
852 amylopectin. *Plant Physiol*, **138**, 184-195.
853 Wattebled F., Planchot V., Dong Y., Szydlowski N., Pontoire B., Devin A., Ball S. &
854 D'Hulst C. (2008) Further evidence for the mandatory nature of polysaccharide
855 debranching for the aggregation of semicrystalline starch and for overlapping
856 functions of debranching enzymes in Arabidopsis leaves. *Plant Physiol*, **148**, 1309-
857 1323.
858 Yao Y., Thompson D.B. & Guiltinan M.J. (2004) Maize starch-branching enzyme isoforms
859 and amylopectin structure. In the absence of starch-branching enzyme IIb, the
860 further absence of starch-branching enzyme Ia leads to increased branching. *Plant*
861 *Physiol.*, **136**, 3515-3523.
862

863 **TABLES**

864

865 **Table 1:** The branching degree was calculated according to (Szydlowski *et al.*, 2011). The
866 $\lambda_{max}$ of the iodine-amylopectin complex was determined after insoluble polyglucans
867 fractionation by SEC on CL-2B matrix (Figure 8). It was determined at the fraction of
868 maximum absorbance. The crystallinity index and allomorph were determined by wide-
869 angle X-ray scattering. All samples were of B-type. The values are the means of two
870 independent assays. In the case of the *isa1 isa3 pu1* triple mutant, the branching degree was
871 determined for phytoglycogen. NA = not available.

| **Sample** | **WT** | **β1** | **β12** | **β20** | ***isa1 isa3 pu1*** |
|---|---|---|---|---|---|
| Branching degree (%) | 5.1 | 6.1 | 6.8 | 7.3 | 8.1 |
| $\lambda_{max}$ of amylopectin (nm) | 563 | 572 | 553 | 552 | NA |
| Crystallinity index (%) | 33 | 27 | 20 | 13 | NA |

872

873 **FIGURE LEGENDS**

874 **Figure 1: Iodine staining of individual plants harvested at the end of the day.** 2-
875 week old plants were harvested and stained with iodine solution after being destained in hot
876 ethanol. All pictures are at the same scale. Colors and intensity of the stain is indicative of
877 the polyglucan content and structure. Wild-type (WT) plants stain dark brown because of
878 the synthesis of high amount of normal starch (ecotype *Wassilewkija*). The *be2 be3* plants
879 stain yellow as a consequence of the lack of any polyglucan in this mutant (Dumez *et al.*,
880 2006). *isa1 isa3 pu1* is a debranching enzyme triple mutant accumulating high amount of
881 phytoglycogen (Wattebled *et al.*, 2008) and therefore stains orange with iodine. β1, β5, β6,
882 β12 and β20 are hygromycin resistant plants selected after transformation of the *be2 be3*
883 mutant with a vector containing the *E. coli glgB* gene. Intermediate colors between those of
884 the WT and the *isa1 isa2* mutant were obtained suggesting that polyglucan synthesis is
885 partially restored in these transgenic lines.

886 **Figure 2: Expression of glgB in the *be2 be3* transformed lines.** (A) Immunoblot
887 analysis performed in denaturing conditions. Protein extracts were denatured before and
888 during migration in the polyacrylamide gel. After migration, proteins were blotted onto a
889 nitrocellulose membrane and hybridized with a peptide-directed antibody raised against
890 GlgB. (B) zymogram of branching enzyme activity. The polyacrylamide gel contains DP7
891 maltooligosaccharides and phosphorylase "a". Branching enzyme activity was revealed by
892 incubating the gel for 2 hours in a phosphorylase "a" stimulating buffer. Bands of branched
893 polyglucans were detected by soaking the gel in iodine solution. (C) Immunoblot analysis
894 performed in non-denaturing conditions: protein extract preparation and migration in the
895 gel was carried out as in (B). After migration, proteins were treated as in (A). WT: wild
896 type of *A. thaliana* (*Wassilewskija* ecotype); β1, β12, β20: transgenic plants expressing
897 GlgB; *be2 be3*: branching enzyme double mutant (Dumez et *al*., 2006); *E. coli*: bacterial
898 cell extract of wild type *E. coli*. Proteins or activity bands corresponding to GlgB expressed
899 in plants were labeled as a, b , and c. In (A), (B) and (C) all lines are from the same gel and
900 blots. (D) *in vitro* assay of branching enzyme activity. Protein extracts were incubated for
901 10 to 40 min in a buffer containing DP7 maltooligosaccharides, phosphorylase "a" and [U-

902 $^{14}$C]Glc-1-P (7.4 kBq per assay) at 50 mM final concentration. The mean of incorporated
903 Glc into branched polyglucans was calculated for 3 independent assays and plotted against
904 the time of incubation. Vertical lines stand for standard deviation. Open diamonds: WT
905 extract; closed squares: *be2 be3* mutant; closed circles: β1; open triangles: β5; closed
906 triangles: β6; open squares: β12; open circles: β20.

907 **Figure 3: Leaf glucan contents.** Glucans were extracted from leaves of 3-week old
908 plants by the perchloric acid protocol. Leaves were harvested at the end of 16-h light
909 period. Insoluble and soluble polyglucans and sugars/maltooligosaccharides were assayed
910 by a spectrophotometric method. The averages of three independent cultures are presented.
911 WT: wild type *WS* ecotype; β1, β12, β20: transgenic plants expressing the *E. coli glgB*
912 gene. Vertical thin bars are the standard deviation of three independent biological
913 replicates.

914 **Figure 4: Transmission electron microscopy of leaf chloroplasts.** Leaves from
915 plants were harvested at the end of the day, cut in small strips and immediately fixed with
916 glutaraldehyde in a cacodylate buffer and stained with PATAg to reveal glucans. A: wild
917 type from *Wassilewskija* ecotype of *A. thaliana*; B: *be2 be3*: branching enzyme double
918 mutant; C: *isa1 isa3 pu1*: debranching enzyme triple mutant accumulating phytoglycogen
919 (Wattebled *et al.*, 2008); D: β1, E: β12, F: β20: *be2 be3* transgenic plants expressing the
920 bacterial *glgB* gene.

921 **Figure 5: Scanning electron microscopy of purified insoluble polyglucans.**
922 Insoluble polyglucans were extracted and purified from leaves of 3-week-old plants
923 harvested at the end of the day of 16-h light / 8 h dark cycles. A: wild-type *Wassilewskija*
924 ecotype; B: β1; C: β12; D: β20 (inset: magnified view of the smallest particles).

925 **Figure 6: Morphology of particles purified from the insoluble polyglucans of**
926 **the GlgB-expressing lines.** TEM images of negatively stained particles from the insoluble
927 fractions of β12 (A, B) and β20 (C, D).

928 **Figure 7: Morphology of particles purified from the soluble polyglucans**
929 **isolated from the GlgB-expressing lines.** TEM images of negatively stained particles
930 from the water-soluble polyglucans isolated from β12 (A) and β20 (B). The image of maize
931 phytoglycogen (C) is given for comparison.

932 **Figure 8: Fractionation of insoluble polyglucans by size exclusion**
933 **chromatography.** Purified insoluble polyglucans were dispersed in DMSO, solubilized in
934 NaOH 10 mM and loaded onto a Sepharose® CL-2B matrix. Elution was conducted in
935 NaOH 10 mM at a rate of 12 $mL.h^{-1}$. 300 µL fractions were collected and subsequently
936 analyzed by iodine spectrophotometry. Thick continuous lines are the maximum
937 absorbance of the iodine-polyglucan complexes (left Y-axis). Dashed lines indicate the
938 wavelength (nm) of the iodine-polyglucan complex at the maximum of absorbance (right
939 Y-axis). X-axis is the volume of elution in mL. A: WT; B: β1; C: β12; D: β20.

940 **Figure 9: Chain length distribution of insoluble polyglucans.** Purified insoluble
941 polyglucans were digested with a mix of bacterial debranching enzymes. The
942 corresponding linear glucans were separated by high-performance anion exchange
943 chromatography and detected by pulsed amperometric detection (HPAEC-PAD). The
944 fraction of each DP (from 3 to 60 glucose residues) is expressed in % of the total DP
945 presented on the profile. (A) WT: continuous black line; β1: grey triangles; β12: closed
946 circles; β20: discontinuous grey line. (B) Comparison of the profiles of the WT (continuous
947 black line) and β20 (discontinuous grey line). The profile of the *isa1 isa3 pu1* triple mutant
948 already published in (Wattebled *et al.*, 2008) is given (open diamonds). (C) Comparison of
949 the profiles of the WT (continuous black line) and β1 (grey triangles).

950 **Figure 10: Starch or starch-like polyglucan synthesis occurs thanks to a**
951 **balanced branching / debranching activity ratio assuming that starch synthase**
952 **activity is not limiting whatever the branching/debranching ratio.** Left panel: in the
953 absence of branching activity (*be2 be3* double mutant), starch or phytoglycogen synthesis is
954 impossible and is substituted by maltose accumulation; the BR/DEBR ratio is null. Middle
955 panel: when the ratio BR/DEBR activity is balanced (WT) or near-balanced (β1), starch or

956 starch-like polyglucan synthesis is promoted. In the case of β1, the slight structural
957 modification of starch is due to the expression of the bacterial glycogen-branching enzyme
958 that has different catalytic and regulatory properties. Right panel: in the absence of
959 debranching activity (such as in *isa1 isa3 pu1*; BR/DEBR is infinite) or when branching
960 activity is extremely high (such as in β20; BR/DEBR >> optimal) phytoglycogen or
961 phytoglycogen-like insoluble polyglucan is synthesized respectively. Superimposed
962 drawings correspond to (from left to right): maltose, amylopectin, phytoglycogen; black
963 points depict the reducing end.

964 **SUPPORTING INFORMATION**

965 Supporting Figure S1: **Description of the approach employed for the synthesis the GlgB**
966 **chimeric sequence used for expression in *A. thaliana*.**

967 Supporting Figure S2: **Comparison of mature plant size.**

968 Supporting Figure S3: **Iodine-staining phenotype of individual plants harvested at**
969 **different time points.**

970 Supporting Figure S4: **Chain length distribution profiles of water-soluble polyglucans.**

971 Supporting Figure S5: **Zymogram analysis of starch and β-limit dextrins hydrolyzing**
972 **enzymes from transformed plants expressing GlgB.**

973 Supporting Figure S6: **Zymogram analysis of soluble starch synthases activities.**

974 Supporting Figure S7: **Structure of polysaccharides produced in β5 and β6**
975 **transformant lines.**

976 Supporting Figure S8: **Leaf glucan contents and granule morphology.**

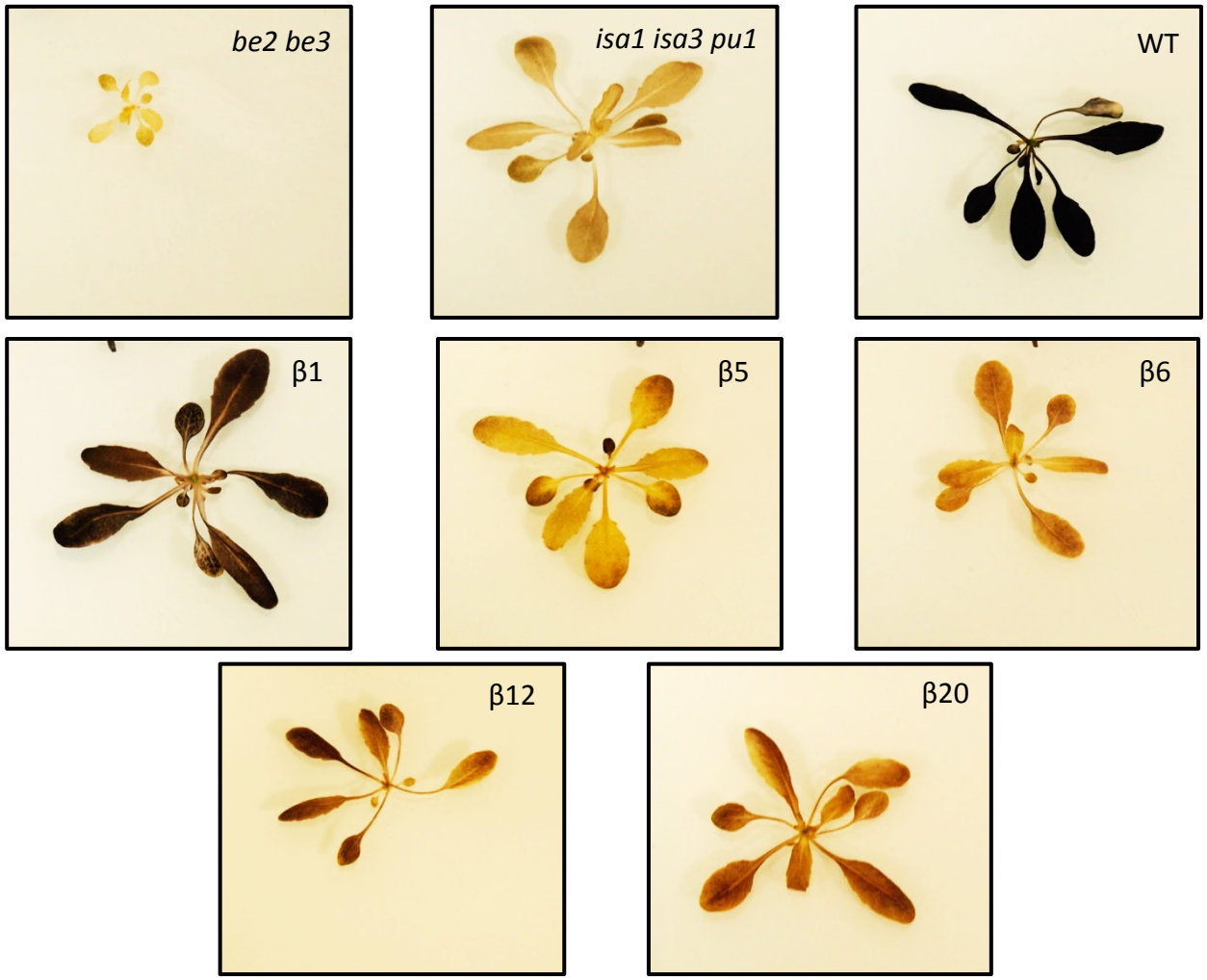


**Figure 1: Iodine staining of individual plants harvested at the end of the day.** 2-week old plants were harvested and stained with iodine solution after being destained in hot ethanol. All pictures are at the same scale. Colors and intensity of the stain is indicative of the polyglucan content and structure. Wild-type (WT) plants stain dark brown because of the synthesis of high amount of normal starch (ecotype *Wassilewkija*). The *be2 be3* plants stain yellow as a consequence of the lack of any polyglucan in this mutant (Dumez et al. 2006). *isa1 isa3 pu1* is a debranching enzyme triple mutant accumulating high amount of phytoglycogen (Wattebled et al. 2008) and therefore stains orange with iodine. β1, β5, β6, β12 and β20 are hygromycin resistant plants selected after transformation of the *be2 be3* mutant with a vector containing the *E. coli glgB* gene. Intermediate colors between those of the WT and the *isa1 isa2* mutant were obtained suggesting that polyglucan synthesis is partially restored in these transgenic lines.

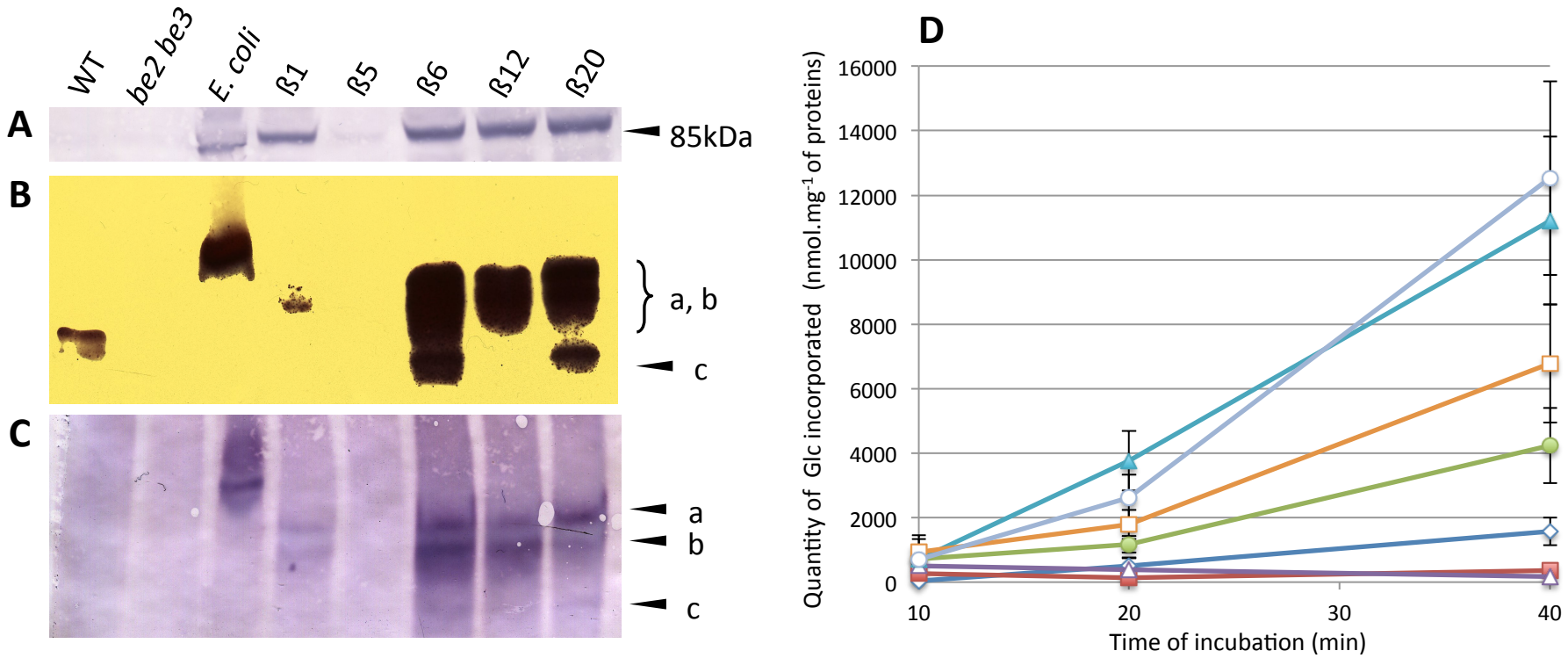


**Figure 2: Expression of *glgB* in the *be2 be3* transformed lines.** (A) Immunoblot analysis performed in denaturing conditions. Protein extracts were denatured before and during migration in the polyacrylamide gel. After migration, proteins were blotted onto a nitrocellulose membrane and hybridized with a peptide-directed antibody raised against GlgB. (B) zymogram of branching enzyme activity. The polyacrylamide gel contains DP7 maltooligosaccharides and phosphorylase "a". Branching enzyme activity was revealed by incubating the gel for 2 hours in a phosphorylase "a" stimulating buffer. Bands of branched polyglucans were detected by soaking the gel in iodine solution. (C) Immunoblot analysis performed in non-denaturing conditions: protein extract preparation and migration in the gel was carried out as in (B). After migration, proteins were treated as in (A). WT: wild type of *A. thaliana* (*Wassilewskija* ecotype); β1, β12, β20: transgenic plants expressing GlgB; *be2 be3*: branching enzyme double mutant (Dumez et *al*., 2006); *E. coli*: bacterial cell extract of wild type *E. coli*. Proteins or activity bands corresponding to GlgB expressed in plants were labeled as a, b , and c. In (A), (B) and (C) all lines are from the same gel and blots. (D) *in vitro* assay of branching enzyme activity. Protein extracts were incubated for 10 to 40 min in a buffer containing DP7 maltooligosaccharides, phosphorylase "a" and [U-$^{14}$C]Glc-1-P (7.4 kBq per assay) at 50 mM final concentration. The mean of incorporated Glc into branched polyglucans was calculated for 3 independent assays and plotted against the time of incubation. Vertical lines stand for standard deviation. Open diamonds: WT extract; closed squares: *be2 be3* mutant; closed circles: β1; open triangles: β5; closed triangles: β6; open squares: β12; open circles: β20.

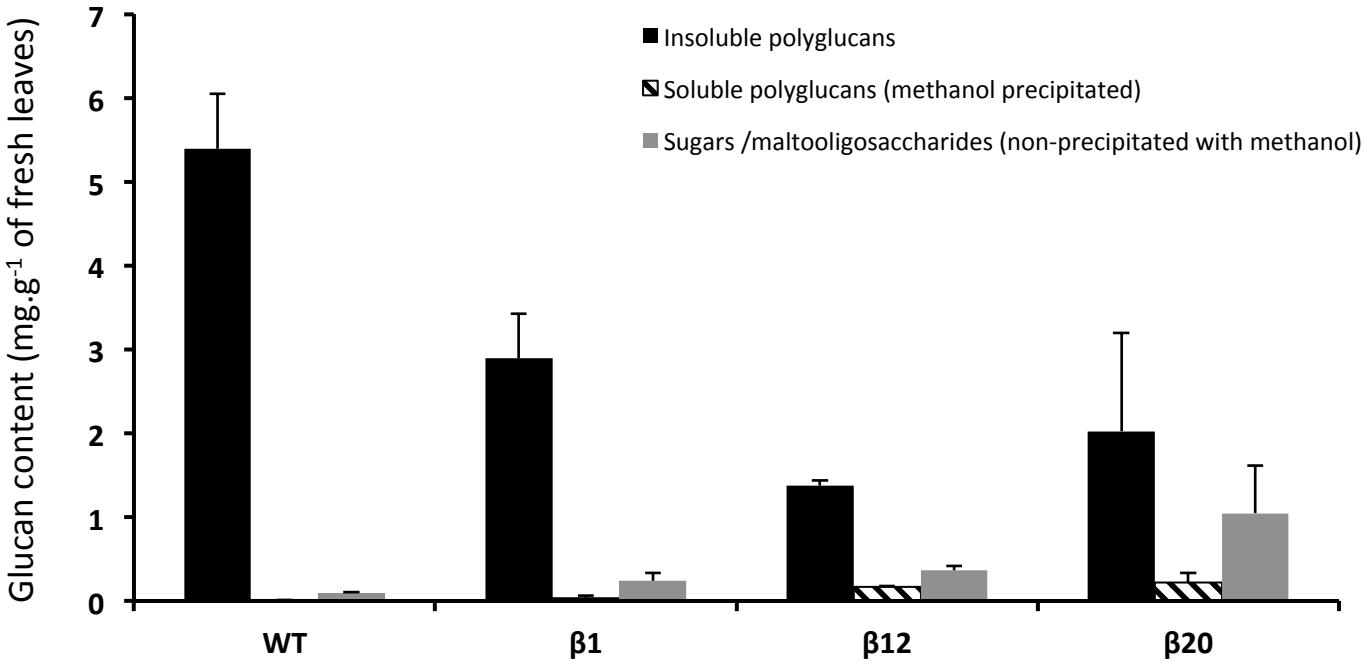


**Figure 3: Leaf glucan contents.** Glucans were extracted from leaves of 3-week old plants by the perchloric acid protocol. Leaves were harvested at the end of 16-h light period. Insoluble and soluble polyglucans and sugars/ maltooligosaccharides were assayed by a spectrophotometric method. The averages of three independent cultures are presented. WT: wild type *WS* ecotype; β1, β12, β20: transgenic plants expressing the *E. coli glgB* gene. Vertical thin bars are the standard deviation of three independent biological replicates.

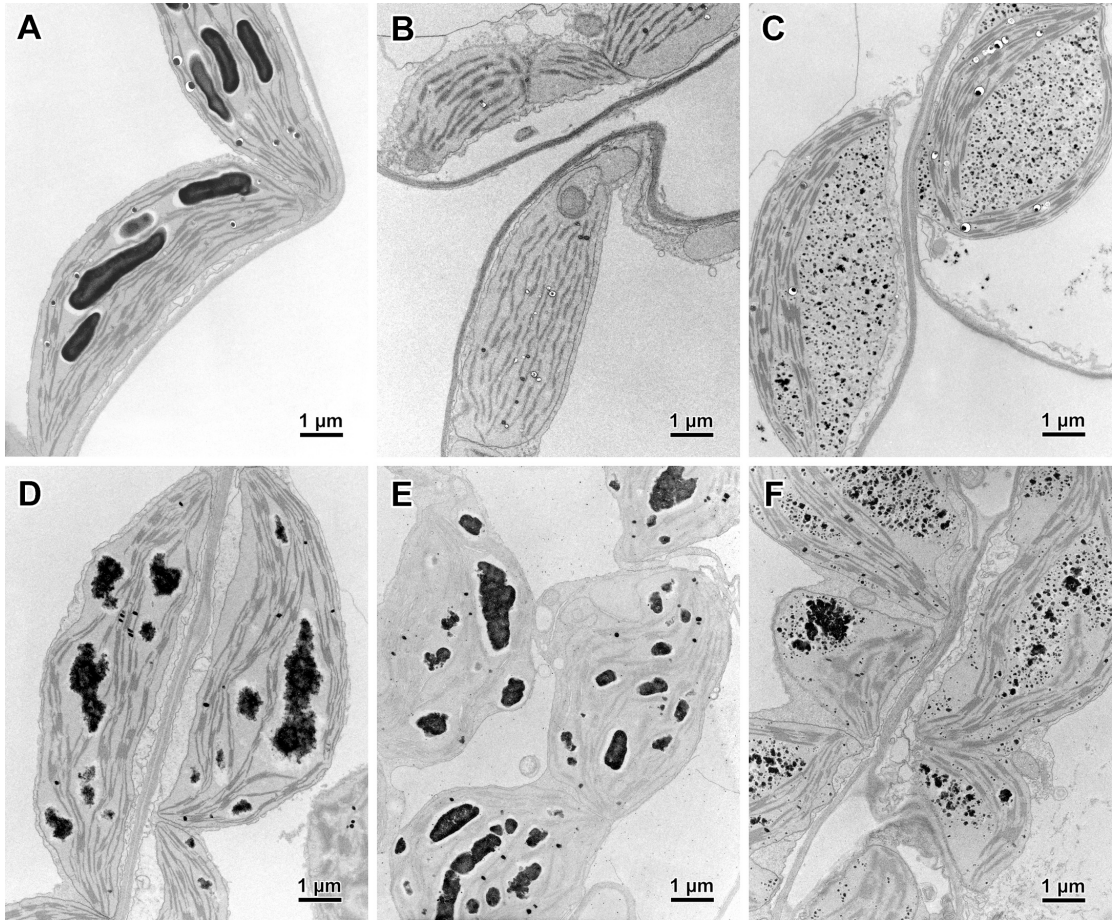


**Figure 4: Transmission electron microscopy of leaf chloroplasts.** Leaves from plants were harvested at the end of the day, cut in small strips and immediately fixed with glutaraldehyde in a cacodylate buffer and stained with PATAg to reveal glucans. A: wild type from *Wassilewskija* ecotype of *A. thaliana*; B: *be2 be3*: branching enzyme double mutant; C: *isa1 isa3 pu1*: debranching enzyme triple mutant accumulating phytoglycogen (Wattebled et al. 2008); D: β1, E: β12, F: β20: *be2 be3* transgenic plants expressing the bacterial *glgB* gene.

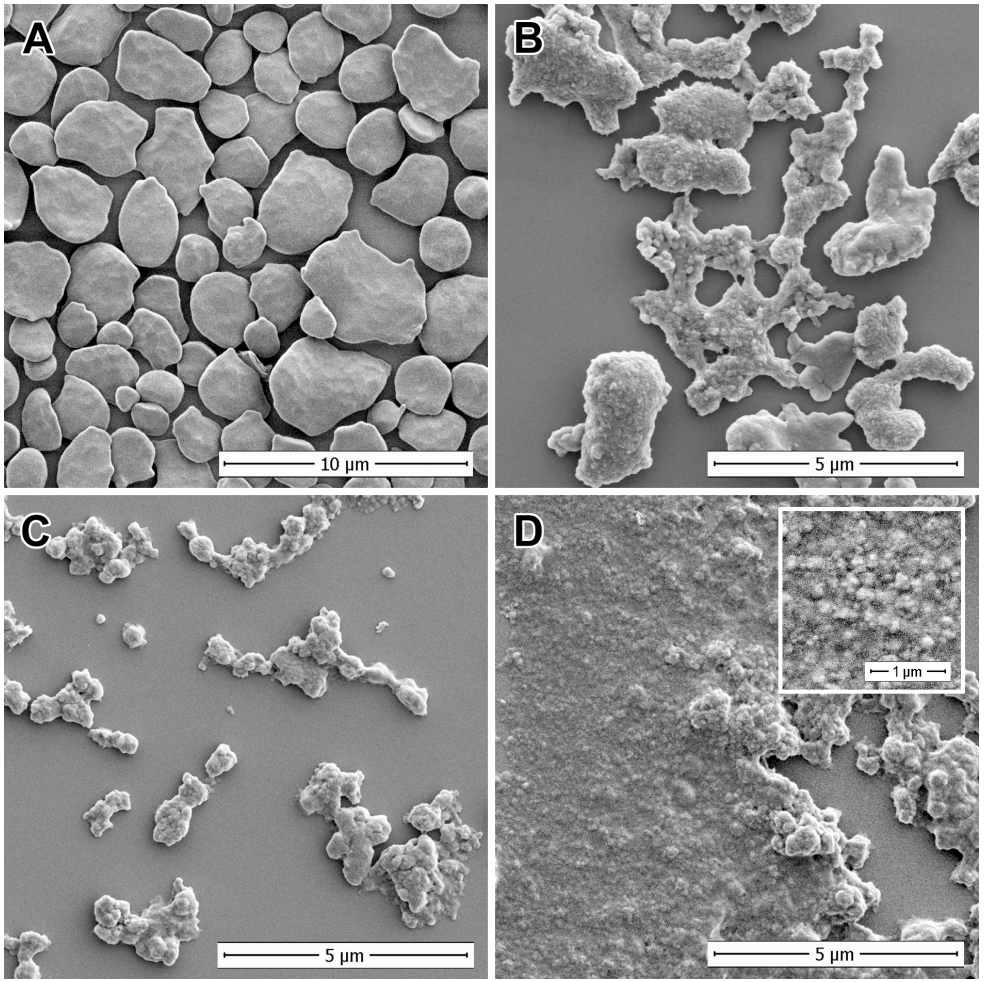


**Figure 5. Scanning electron microscopy of purified insoluble polyglucans.** Insoluble polyglucans were extracted and purified from leaves of 3-week-old plants harvested at the end of the day of 16-h light / 8 h dark cycles. A: wild-type *Wassilewskija* ecotype; B: β1; C: β12; D: β20 (inset: magnified view of the smallest particles).

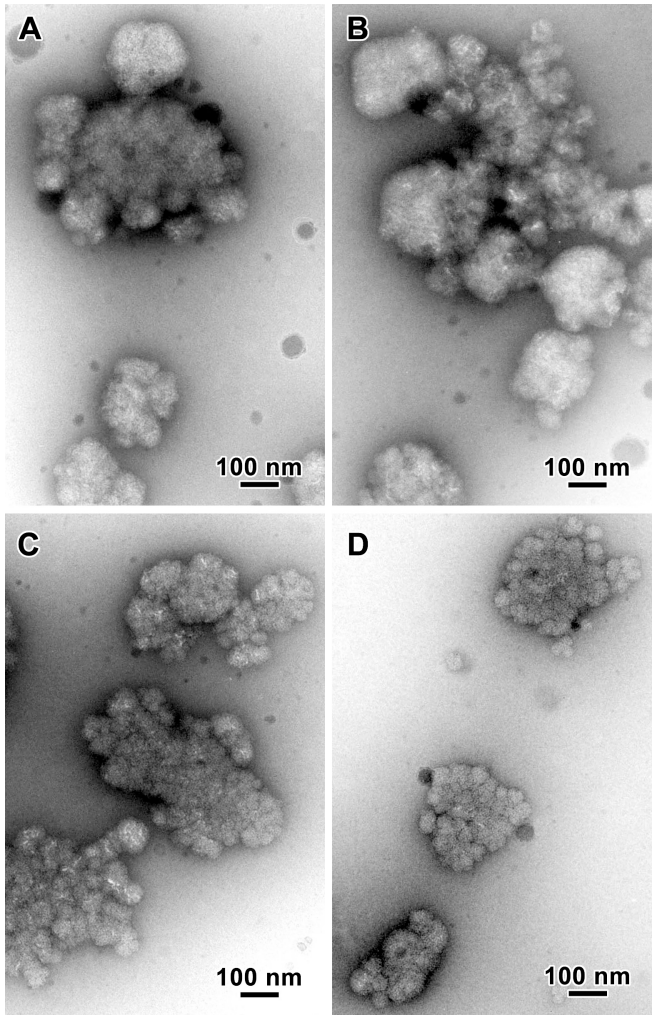


**Figure 6: Morphology of particles purified from the insoluble polyglucans of the GlgB-expressing lines.** TEM images of negatively stained particles from the insoluble fractions of β12 (A, B) and β20 (C, D).

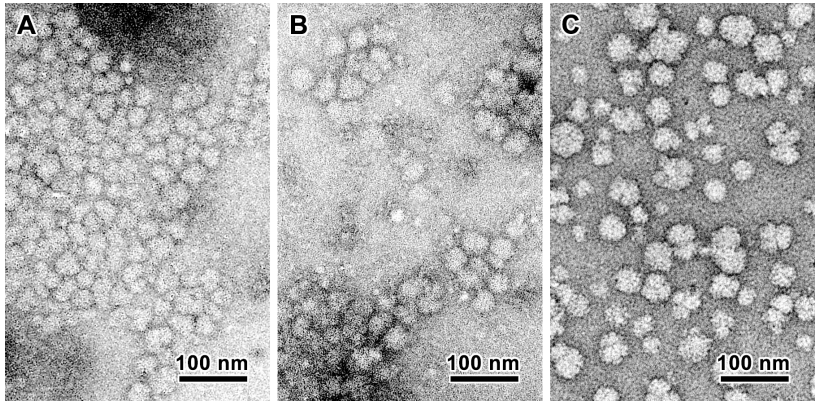


**Figure 7: Morphology of particles purified from the soluble polyglucans isolated from the GlgB-expressing lines.** TEM images of negatively stained particles from the water-soluble polyglucans isolated from β12 (A) and β20 (B). The image of maize phytoglycogen (C) is given for comparison.

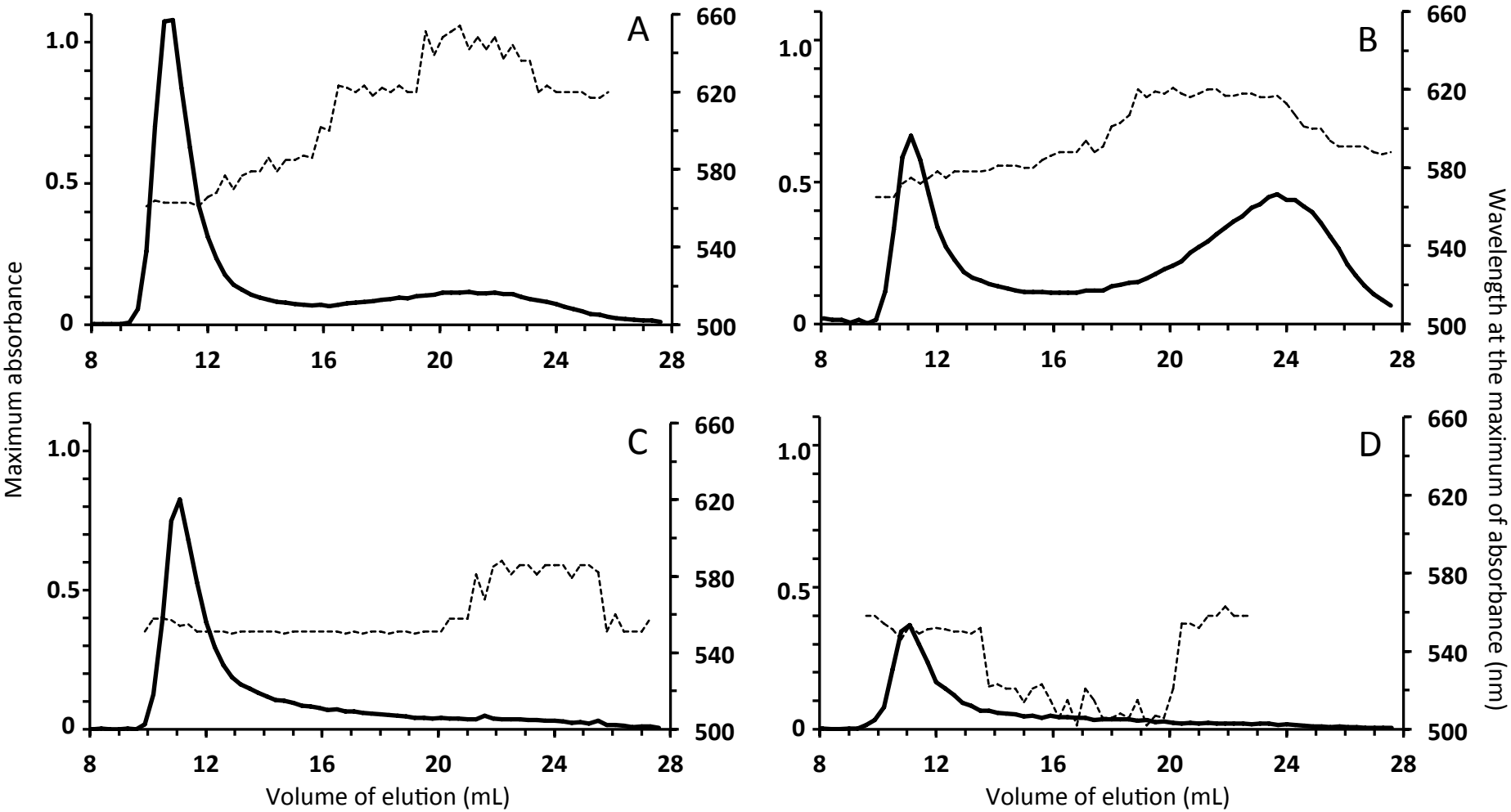


**Figure 8: Fractionation of insoluble polyglucans by size exclusion chromatography.** Purified insoluble polyglucans were dispersed in DMSO, solubilized in NaOH 10 mM and loaded onto a Sepharose® CL-2B matrix. Elution was conducted in NaOH 10 mM at a rate of 12 mL.h$^{-1}$. 300 µL fractions were collected and subsequently analyzed by iodine spectrophotometry. Thick continuous lines are the maximum absorbance of the iodine-polyglucan complexes (left Y-axis). Dashed lines indicate the wavelength (nm) of the iodine-polyglucan complex at the maximum of absorbance (right Y-axis). X-axis is the volume of elution in mL. A: WT; B: β1; C: β12; D: β20.

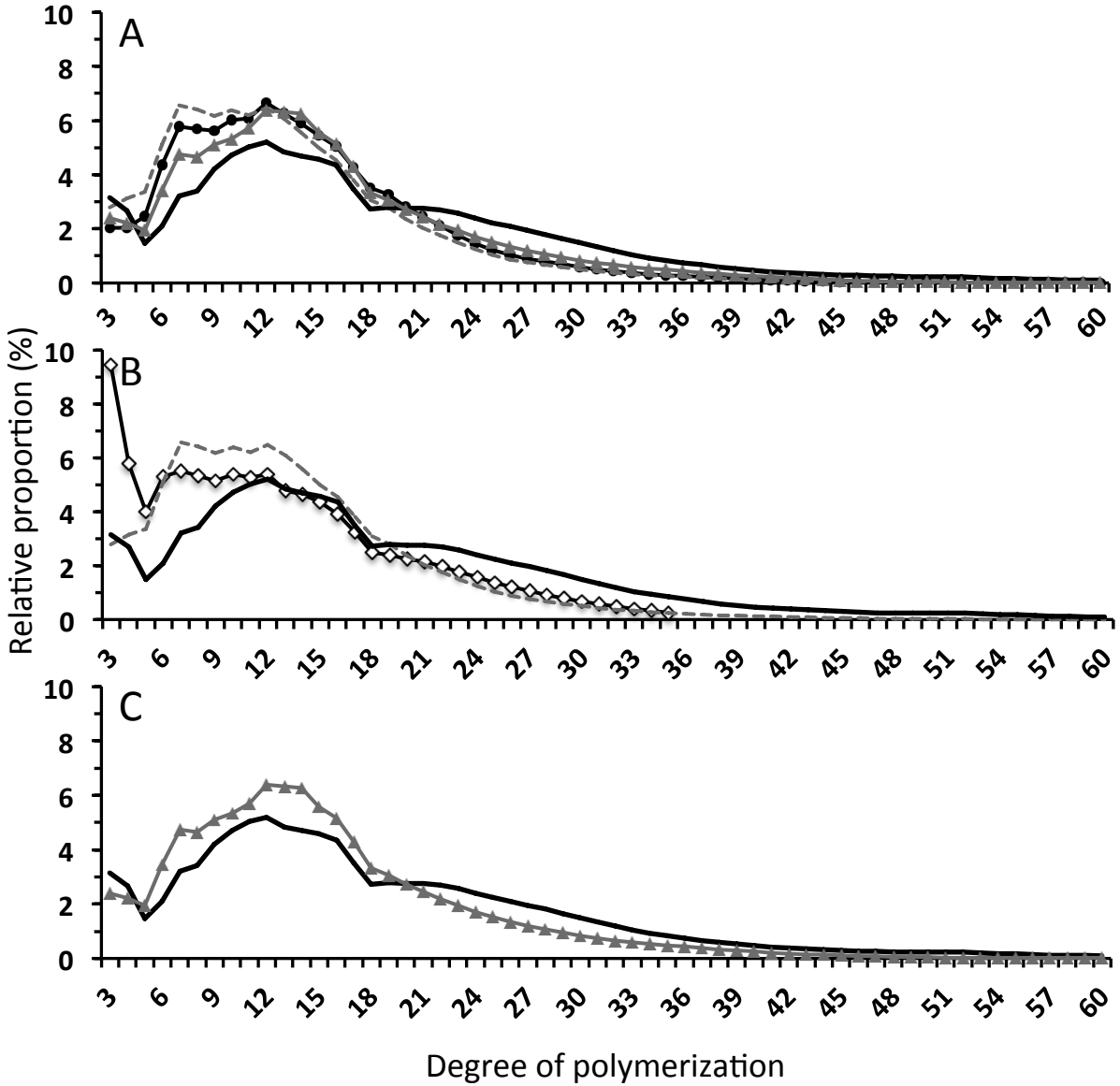


**Figure 9: Chain length distribution of insoluble polyglucans.** Purified insoluble polyglucans were digested with a mix of bacterial debranching enzymes. The corresponding linear glucans were separated by high-performance anion exchange chromatography and detected by pulsed amperometric detection (HPAEC-PAD). The fraction of each DP (from 3 to 60 glucose residues) is expressed in % of the total DP presented on the profile. (A) WT: continuous black line; β1: grey triangles; β12: closed circles; β20: discontinuous grey line. (B) Comparison of the profiles of the WT (continuous black line) and β20 (discontinuous grey line). The profile of the *isa1 isa3 pu1* triple mutant already published in Wattebled et al., 2008 is given (open diamonds). (C) Comparison of the profiles of the WT (continuous black line) and β1 (grey triangles).

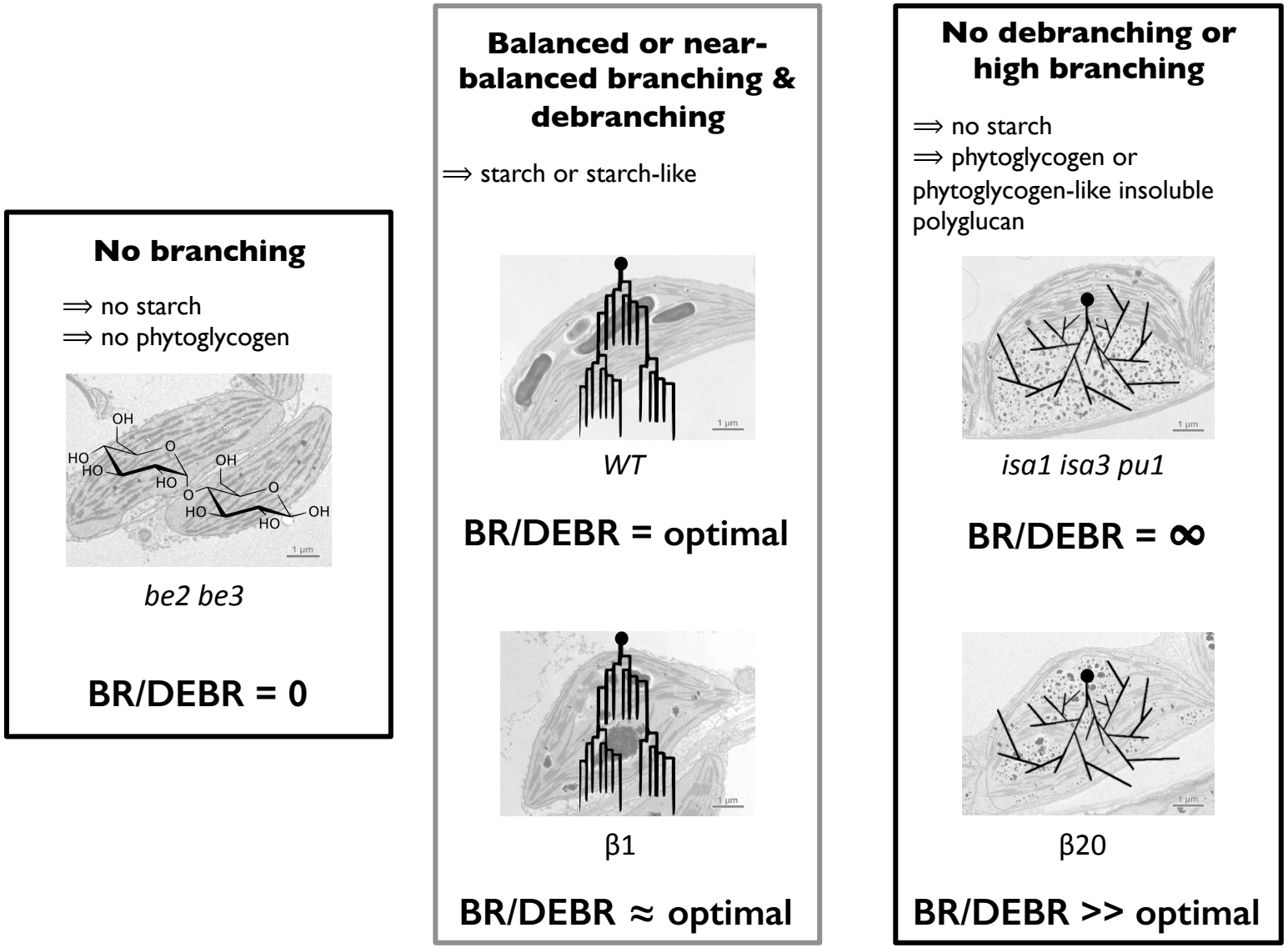


**Figure 10: Starch or starch-like polyglucan synthesis occurs thanks to a balanced branching / debranching activity ratio assuming that starch synthase activity is not limiting whatever the branching/debranching ratio.** Left panel: in the absence of branching activity (*be2 be3* double mutant), starch or phytoglycogen synthesis is impossible and is substituted by maltose accumulation; the BR/DEBR ratio is null. Middle panel: when the ratio BR/DEBR activity is balanced (WT) or near-balanced (β1), starch or starch-like polyglucan synthesis is promoted. In the case of β1, the slight structural modification of starch is due to the expression of the bacterial glycogen-branching enzyme that has different catalytic and regulatory properties. Right panel: in the absence of debranching activity (such as in *isa1 isa3 pu1*; BR/DEBR is infinite) or when branching activity is extremely high (such as in β20; BR/DEBR >> optimal) phytoglycogen or phytoglycogen-like insoluble polyglucan is synthesized respectively. Superimposed drawings correspond to (from left to right): maltose, amylopectin, phytoglycogen; black points depict the reducing end.

**Supplemental Figure S1**

**Description of the approach employed for the synthesis the GlgB chimeric sequence used for expression in *A. thaliana*.**

The chimeric sequence used to transform the *be2 be3* double mutant is composed of the nucleotide sequence of the transit peptide of the plant gene AtBE2 (At5g03650) and the E. coli *glgB* nucleotide sequence (M13751). a) Global scheme of the method is presented. b) Primers nucleotide sequences. Nucleotides in green correspond to the AtBE2 transit peptide sequence and nucleotides in red correspond to the coding sequence of *glgB*. Nucleotides "CACC" highlighted in blue are required for insertion of the sequence in the pENTR/D-TOPO vector. (c) Hybridization temperatures used for each couple of primers and number of cycles used during amplification. (d) Nucleotide and amino acid sequences of the chimeric gene.

## a) Global scheme

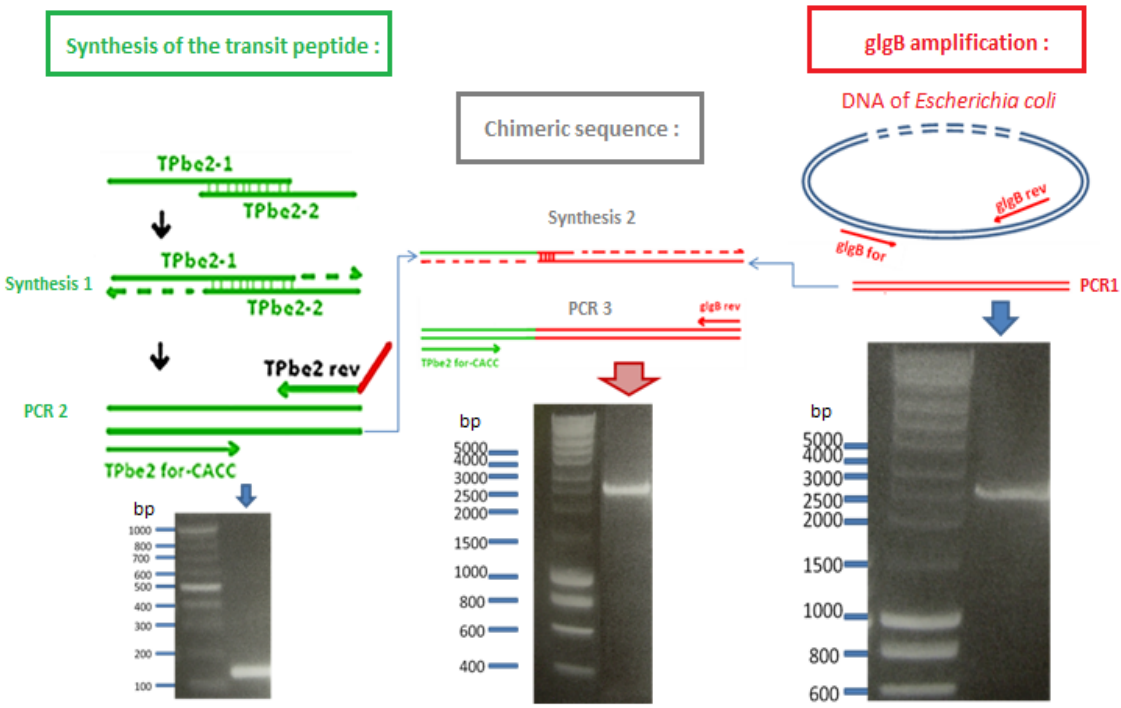


The coding sequence of *glgB* was amplified directly with *E. coli* genomic DNA (PCR1). The transit peptide was synthesized with two long complementary primers (synthesis 1) (PCR2). PCR products 1 and 2 were hybridized to synthesize the chimeric sequence (synthesis 2) and the chimeric sequence was finally amplified (PCR 3) before its insertion in the entry vector.

### b) Primers sequences

| | |
|---|---|
| **glgB for** | atgtccgatcgtatcgatagagacgtgatt |
| **glgB rev** | tcattctgcctcccgaacca |
| **TPbe2-1** | atggtggtgattcacggagtgtctcttactccacgcttcactcttccttctcgacctc tcaacactggctttaatgccggcaattccaccctctctttcttcttcaaaaagcaccc tc |
| **TPbe2-2** | agagatagcttgtgacgaagaatcaaactccgcagattgtttcccagcaaagatcttc cgagagagagggtgctttttgaagaagaaagagagggtgg |
| **TPbe2 for-CACC** | caccatggtggtgattcacggagt |
| **TPbe2 rev** | aatcacgtctctatcgatacgatcggacatagagatagcttgtgacgaagaatca |

### c) PCR conditions

| Primer couples | Hybridization temperatures | Number of cycles |
|---|---|---|
| **PCR1: glgB for / glgB rev** | 61°C | 34 |
| **SYNTHESIS 1: TPbe2-1 / TPbe2-2** | 55°C | 24 |
| **PCR2: TPbe2 for-CACC / Tpbe2 rev** | 54°C | 30 |
| **SYNTHESIS 2: with amplicons from PCR1 & PCR2** | 54°C | 20 |
| **PCR3: TPbe2 for-CACC / glgB rev** | 54°C | 34 |

### d) Chimeric sequences

Nucleotide sequence of the chimeric gene

In green: nucleotides corresponding to the transit peptide of the AtBE2 gene. In red: nucleotides of the coding sequence of *E. coli glgB* gene. In blue, nucleotides required for insertion of the construction into the entry vector. Underlined nucleotides correspond to the primers used for PCR amplification (see table above)

CACCATGGTGGTGATTCACGGAGTGTCTCTTACTCCACGCTTCACTCTTCCTTCTCGACCTCTCAA
CACTGGCTTTAATGCCGGCAATTCCACCCTCTCTTTCTTCTTCAAAAAGCACCCTCTCTCTCGGAA
GATCTTTGCTGGGAAACAATCTGCGGAGTTTGATTCTTCGTCACAAGCTATCTCTATGTCCGATCG
TATCGATAGAGACGTGATTAACGCGCTAATTGCAGGCCATTTTGCGGATCCTTTTTCCGTACTGGG
AATGCATAAAACCACCGCGGGACTGGAAGTCCGTGCCCTTTTACCCGACGCTACCGATGTGTGGGT
GATTGAACCGAAAACCGGGCGCAAACTCGCAAAACTGGAGTGTCTCGACTCACGGGGATTCTTTAG
CGGCGTCATTCCGCGACGTAAGAATTTTTTCCGCTATCAGTTGGCTGTTGTCTGGCATGGTCAGCA
AAACCTGATTGATGATCCTTACCGTTTTGGTCCGCTAATCCAGGAAATGGATGCCTGGCTATTATC
TGAAGGTACTCACCTGCGCCCGTATGAAACCTTAGGCGCGCATGCAGATACTATGGATGGCGTCAC
AGGTACGCGTTTCTCTGTCTGGGCTCCAAACGCCCGTCGGGTCTCGGTGGTTGGGCAATTCAACTA
CTGGGACGGTCGCCGTCACCCGATGCGCCTGCGTAAAGAGAGCGGCATCTGGGAACTGTTTATCCC
TGGGGCGCATAACGGTCAGCTCTATAAATACGAGATGATTGATGCCAATGGCAACTTGCGTCTGAA
GTCCGACCCTTATGCCTTTGAAGCGCAAATGCGCCCGGAAACCGCGTCTCTTATTTGCGGGCTGCC
GGAAAAGGTTGTACAGACTGAAGAGCGCAAAAAAGCGAATCAGTTTGATGCGCCAATCTCTATTTA
TGAAGTTCACCTGGGTTCCTGGCGTCGCCACACCGACAACAATTTCTGGTTGAGCTACCGCGAGCT
GGCCGATCAACTGGTGCCTTATGCTAAATGGATGGGCTTTACCCACCTCGAACTACTGCCCATTAA
CGAGCATCCCTTCGATGGCAGTTGGGGTTATCAGCCAACCGGCCTGTATGCGCCAACCCGCCGTTT

TGGTACTCGCGACGACTTCCGTTATTTCATTGATGCCGCACACGCAGCTGGTCTGAACGTGATTCT
CGACTGGGTGCCAGGCCACTTCCCGACTGATGACTTTGCGCTTGCCGAATTTGATGGCACGAACTT
GTATGAACACAGCGATCCGCGTGAAGGCTATCATCAGGACTGGAACACGCTGATCTACAACTATGG
TCGCCGTGAAGTCAGTAACTTCCTCGTCGGTAACGCGCTTTACTGGATTGAACGTTTTGGTATTGA
TGCGCTGCGCGTCGATGCGGTGGCGTCAATGATTTATCGCGACTACAGCCGTAAAGAGGGGGAGTG
GATCCCGAACGAATTTGGCGGGCGCGAGAATCTTGAAGCGATTGAATTCTTGCGTAATACCAACCG
TATTCTTGGTGAGCAGGTTTCCGGTGCGGTGACAATGGCTGAGGAGTCTACCGATTTCCCTGGCGT
TTCTCGTCCGCAGGATATGGGCGGTCTGGGCTTCTGGTACAAGTGGAACCTCGGCTGGATGCATGA
CACCCTGGACTACATGAAGCTCGACCCGGTTTATCGTCAGTATCATCACGATAAACTGACCTTCGG
GATTCTCTACAACTACACTGAAAACTTCGTCCTGCCGTTGTCGCATGATGAAGTGGTCCACGGTAA
AAAATCGATTCTCGACCGCATGCCGGGCGACGCATGGCAGAAATTCGCGAACCTGCGCGCCTACTA
TGGCTGGATGTGGGCATTCCCGGGCAAGAAACTACTGTTCATGGGTAACGAATTTGCCCAGGGCCG
CGAGTGGAACCATGACGCCAGCCTCGACTGGCATCTGTTGGAAGGCGGCGATAACTGGCACCACGG
TGTCCAGCGTCTGGTGCGCGATCTGAACCTCACCTACCGCCACCATAAAGCAATGCATGAACTGGA
TTTTGACCCGTACGGCTTTGAATGGCTGGTGGTGGATGACAAAGAACGCTCGGTGCTGATCTTTGT
GCGTCGCGATAAAGAGGGTAACGAAATCATCGTTGCCAGTAACTTTACGCCGGTACCGCGTCATGA
TTATCGCTTCGGCATAAACCAGCCGGGCAAATGGCGTGAAATCCTCAATACCGATTCCATGCACTA
TCACGGCAGTAATGCAGGCAATGGCGGCACGGTACACAGCGATGAGATTGCCAGCCACGGTCGTCA
GCATTCACTAAGCCTGACGCTACCACCGCTGGCCACTATCTGGCTGGTTCGGGAGGCAGAATGA

Aminoacid sequence of the chimeric GlgB protein (transit peptide in green)

MVVIHGVSLTPRFTLPSRPLNTGFNAGNSTLSFFFKKHPLSRKIFAGKQSAEFDS
SSQAISMSDRIDRDVINALIAGHFADPFSVLGMHKTTAGLEVRALLPDATDVWVI
EPKTGRKLAKLECLDSRGFFSGVIPRRKNFFRYQLAVVWHGQQNLIDDPYRFGPL
IQEMDAWLLSEGTHLRPYETLGAHADTMDGVTGTRFSVWAPNARRVSVVGQFNYW
DGRRHPMRLRKESGIWELFIPGAHNGQLYKYEMIDANGNLRLKSDPYAFEAQMRP
ETASLICGLPEKVVQTEERKKANQFDAPISIYEVHLGSWRRHTDNNFWLSYRELA
DQLVPYAKWMGFTHLELLPINEHPFDGSWGYQPTGLYAPTRRFGTRDDFRYFIDA
AHAAGLNVILDWVPGHFPTDDFALAEFDGTNLYEHSDPREGYHQDWNTLIYNYGR
REVSNFLVGNALYWIERFGIDALRVDAVASMIYRDYSRKEGEWIPNEFGGRENLE
AIEFLRNTNRILGEQVSGAVTMAEESTDFPGVSRPQDMGGLGFWYKWNLGWMHDT
LDYMKLDPVYRQYHHDKLTFGILYNYTENFVLPLSHDEVVHGKKSILDRMPGDAW
QKFANLRAYYGWMWAFPGKKLLFMGNEFAQGREWNHDASLDWHLLEGGDNWHHGV
QRLVRDLNLTYRHHKAMHELDFDPYGFEWLVVDDKERSVLIFVRRDKEGNEIIVA
SNFTPVPRHDYRFGINQPGKWREILNTDSMHYHGSNAGNGGTVHSDEIASHGRQH
SLSLTLPPLATIWLVREAE

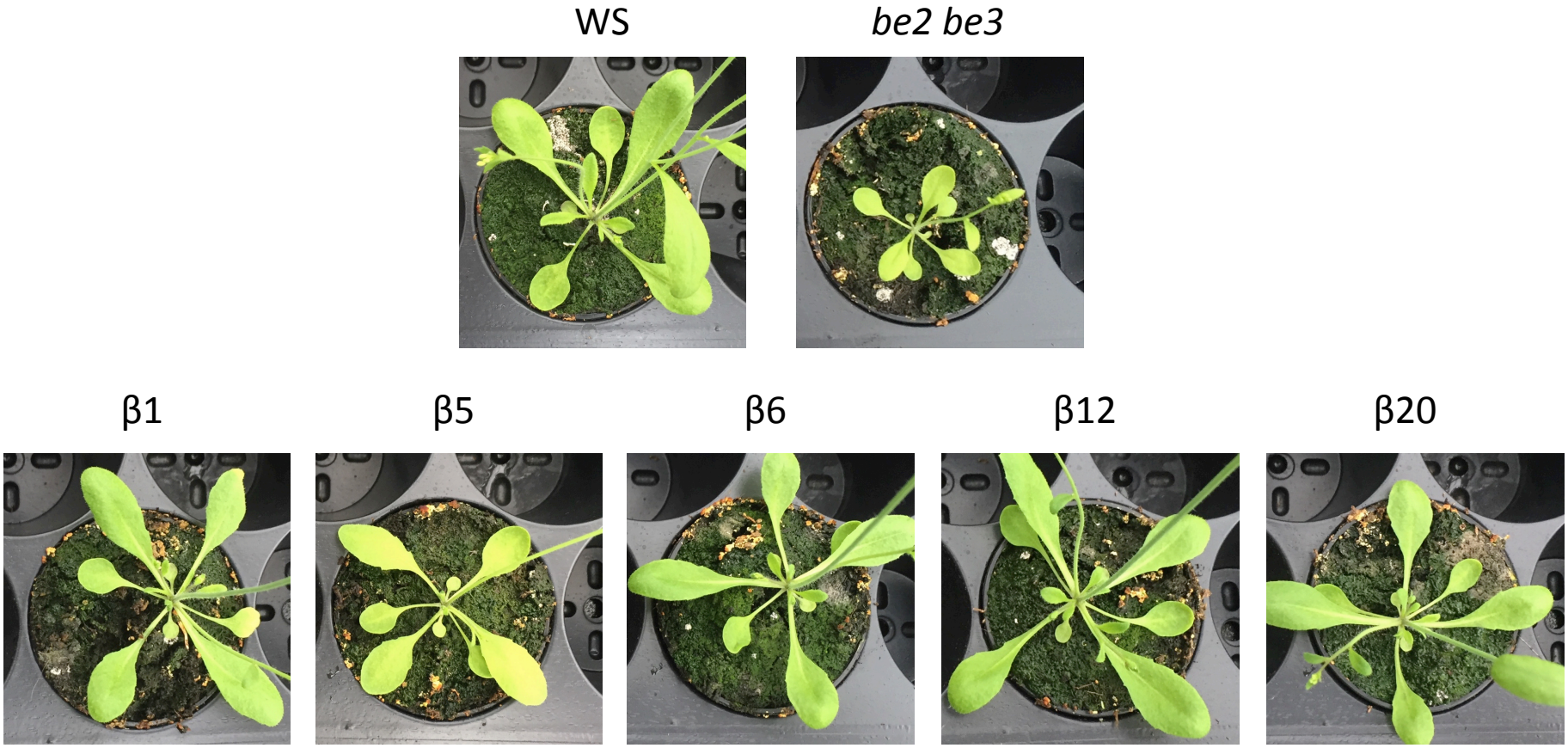


**Supplemental Figure S2: comparison of mature plant size.** Seeds were sown on peat-based compost and plants were grown in greenhouse for 16h in the light at 21°C and 8h in the dark and 16°C. Pictures were taken 3 weeks after germination. The *be2 be3* double mutant has a strong growth retardation phenotype and plants are much smaller than wild type (Dumez et al., 2006) whereas all transformed plants expressing *E. coli* GlgB branching enzyme have a phenotype close to that of the wild type reference.

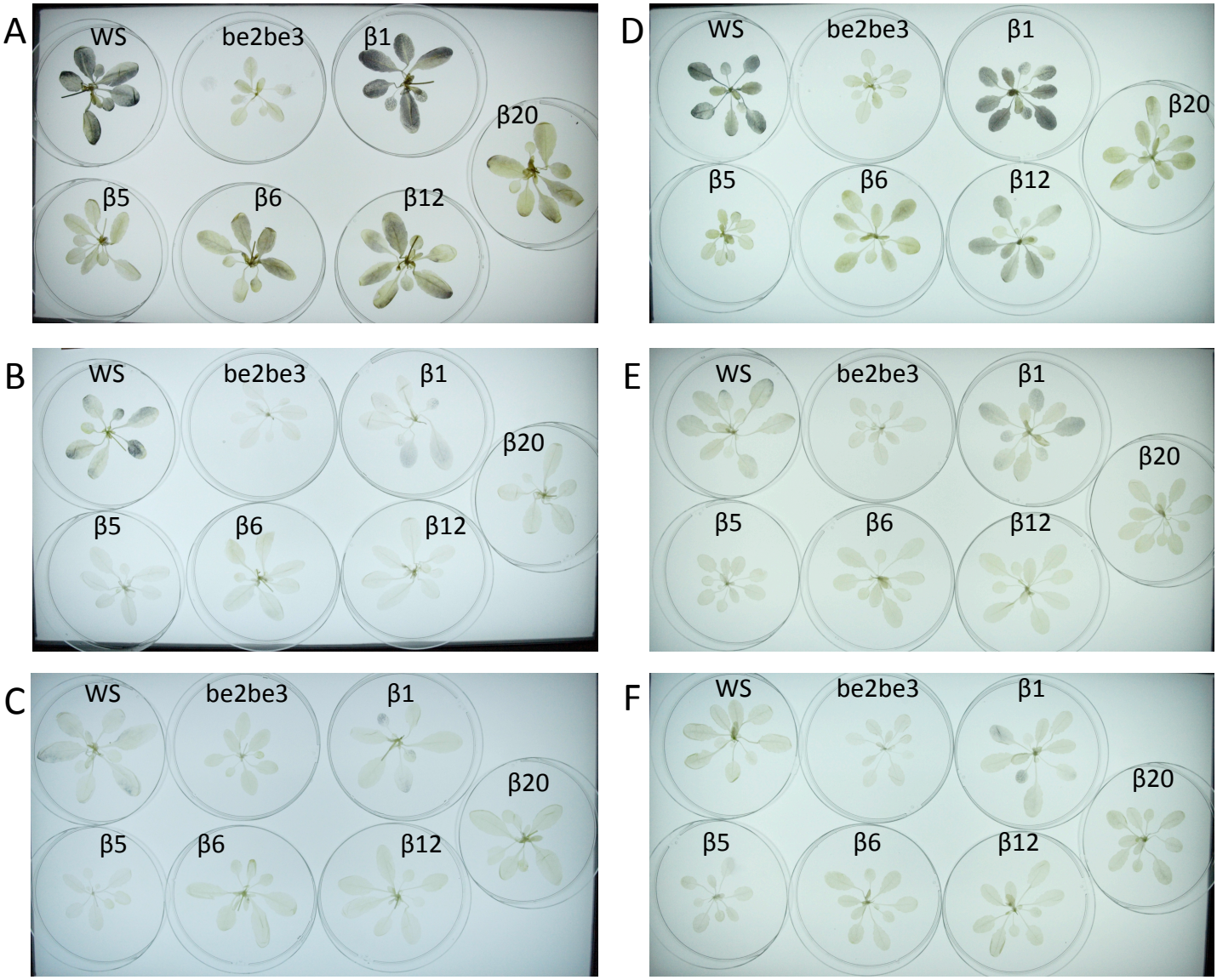


**Supplemental Figure S3: Iodine-staining phénotype of individual plants harvested at different time points.** Plants were cultivated in growth cabinet in 16-h light; 8-h dark (A, B, C) or in 12-h light; 12-h dark (D, E, F) regime at 23°C during the day and 20°C during the night and 100 $\mu E.m^{-2}.s^{-1}$ irradiance. Plants were harvested at the end of light period (A and D) or at the end of the dark period (B and E). In panels C and F plants were left 24 more hours in the dark. All plants were destained in hot ethanol and stained with iodine solution. At the end of the dark period (Panels B and E) polysaccharide degradation is either complete (β5, β6, β12, β20;) or similar to the wild type line (β1). After an extend of 24 hours in darkness, all lines appear colorless.

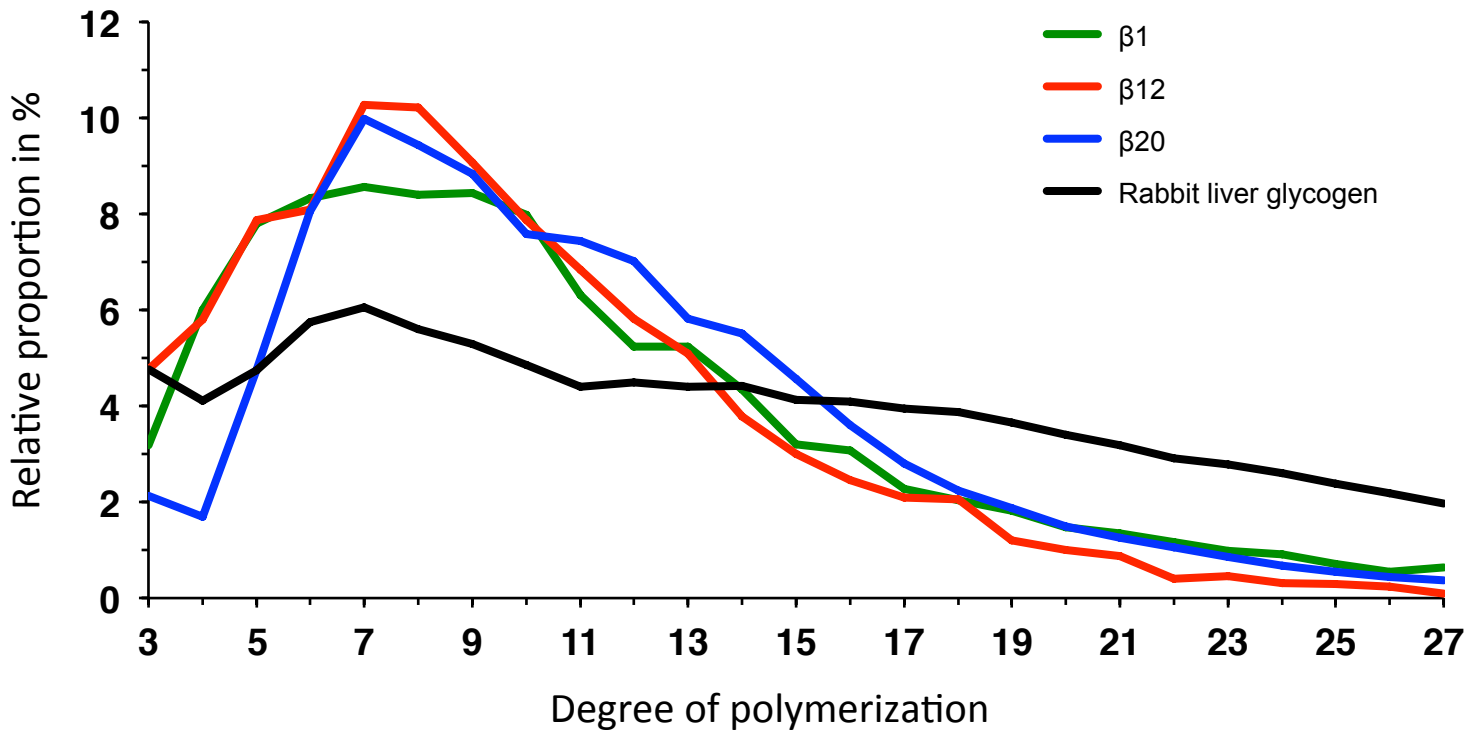


**Supplemental Figure S4: Chain length distribution profiles of water soluble polyglucans** purified from GlgB-expressing lines β1 (green), β12 (red) and β20 (blue) compared to that of the rabbit liver glycogen (black). After purification, water soluble polyglucans were debranched by a mix of bacterial isoamylase and pullulanase. The branched products were analyzed by HPAEC-PAD. The relative proportion of each glucan is plotted versus their degree of polymerization. Values are the mean of two analysis carried out with soluble polyglucans extracted of plants cultivated independently.

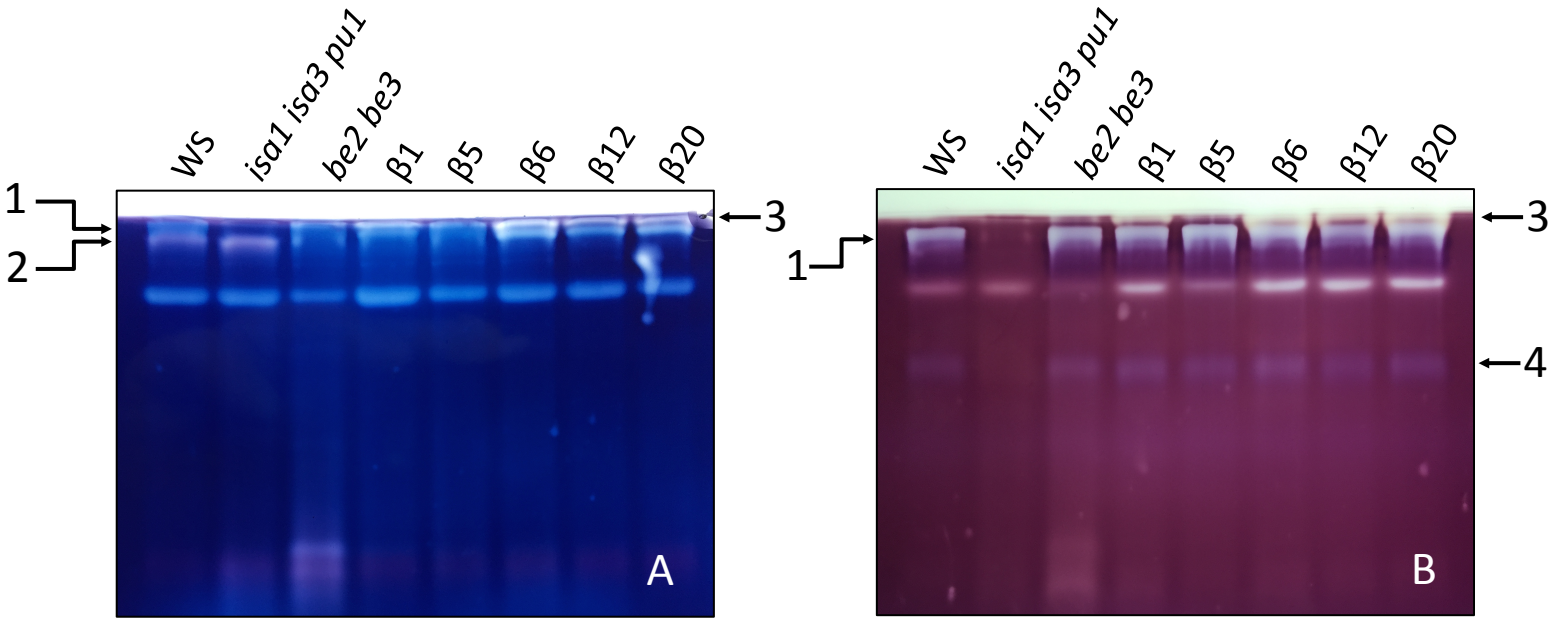


**Supplemental Figure S5: Zymogram analysis of transformed plant expressing GlgB.** Three to four leaves of 3 week-old plants were harvested at mid-day for soluble extract preparation. The equivalent of 50 µg of proteins were loaded on polyacrylamide gel impregnated with either 0.3% of potato soluble starch (A) or 0.3% of maize β-limit dextrins (B). After migration (2 h at 4°C, 15 mA / gel), the gels were incubated overnight at room temperature in a buffer composed of : Tris 25 mM; Glycine 192 mM; $MgCl_2$ 1 mM; $CaCl_2$ 1 mM; DTT 10 mM. After incubation, enzymes that modified the substrate were revealed by soaking the gels in iodine solution (1% KI [w/v]; 0.1% $I_2$ [w/v]). The gels were rinsed in water before taking pictures. WS is the wild type reference (*Wassilewskija*) and all other plants are in the same genetic background. *be2 be3* corresponds to a double mutant lacking endogenous branching enzymes. β1, β5, β6, β12, and β20 are *be2 be3* mutants expressing different levels of *E. coli* GlgB. Blue Band labeled 1 and red band labeled 2 were previously determined as Iso1 and BE2 respectively (Dumez et al., 2006; Wattebled et al., 2008). The pale pink band labeled 3 with an extremely low mobility, present only in transformed plants, corresponds to GlgB. Band 4 is the pullulanase (Wattebled et al., 2008).

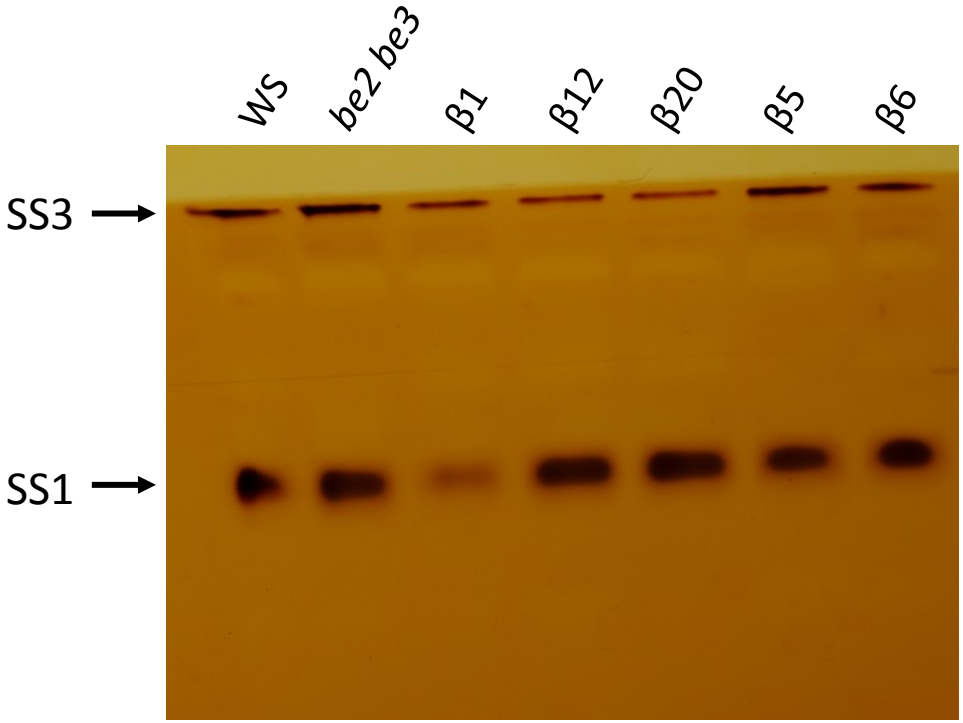


**Supplemental Figure S6: Zymogram analysis of soluble starch synthases activities.** An equal amount of proteins from leaf crude extracts was loaded on native PAGE containing 0.3% (w/v) of rabbit liver glycogen. Approximately 2h30 of migration in native conditions (Tris-glycine buffer 1X, 4°C) was applied. After incubation in an appropriate buffer for starch synthase activity (Glycyl-glycine 66 mM (pH 7.5); $(NH_4)_2SO_4$ 66 mM; $MgCl_2$ 1 mM; β-mercaptoethanol 3.3 mM; ADP-glucose 1.2 mM), the gel was washed 6 times into water to remove β-mercaptoethanol and further incubated in iodine solution until revelation of bands of activity. This zymogram is representative of three biological independent experiments.

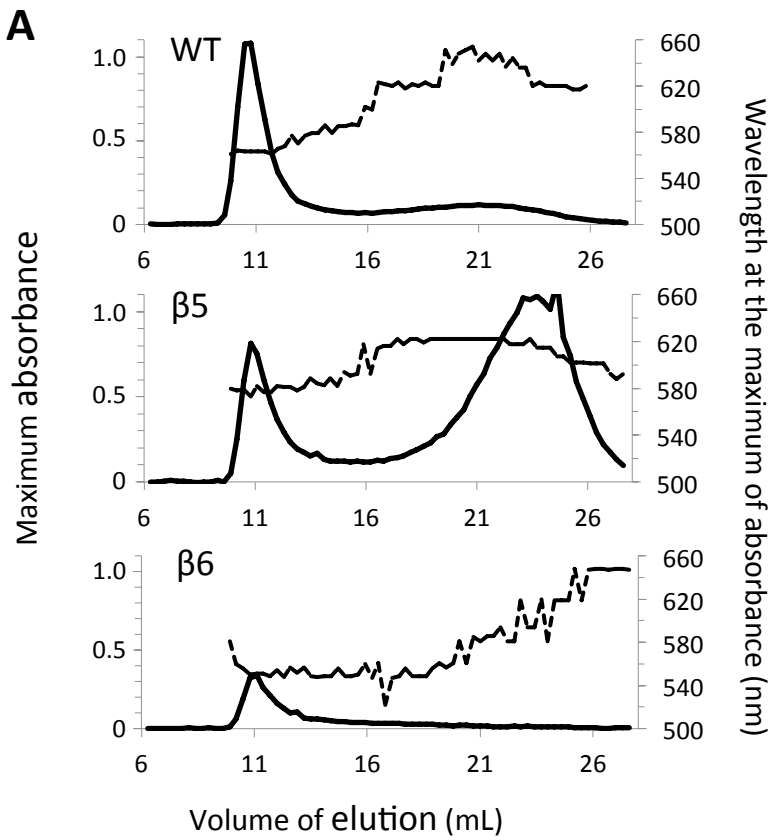


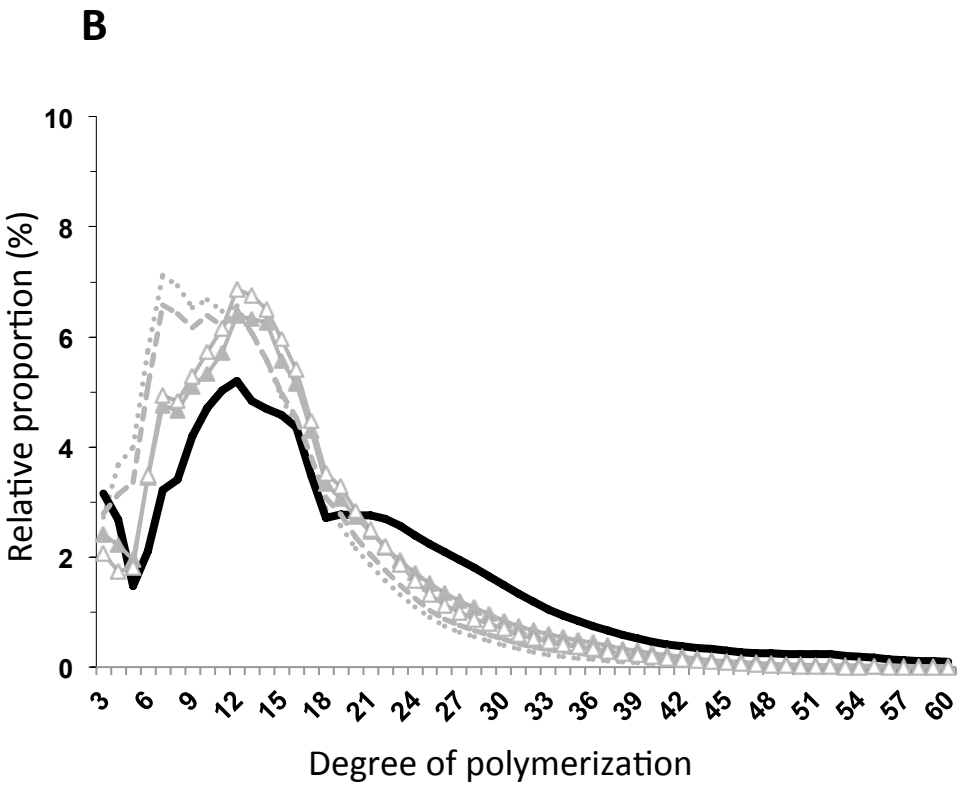


C

| Sample | WT | β5 | β12 | β6 |
|---|---|---|---|---|
| Branching degree (%) | 5.1 | 6.2 | 6.8 | 7.8 |
| $\lambda_{max}$ of amylopectin (nm) | 563 | 571 | 553 | 545 |
| Crystallinity index (%) | 33 | 23 | 20 | 15 |

**Supplemental Figure S7 : Structure of polysaccharides produced in β5 and β6 transformant lines.**

**(A) Fractionation of insoluble polyglucans by size exclusion chromatography.** Dashed lines indicate the wavelength (nm) of the iodine-polyglucan complex at the maximum of absorbance (right Y-axis).

**(B) Chain length distribution of insoluble polyglucans.** WT: continuous black line; β1: closed grey triangles; β5: open grey triangles ; β6: dotted grey line; β20: discontinuous grey line.

**(C) Structural parameters of polysaccharides produced in β5 and β6 tranformant lines**. The branching degree was calculated according to Szydlowski et al. (2011).

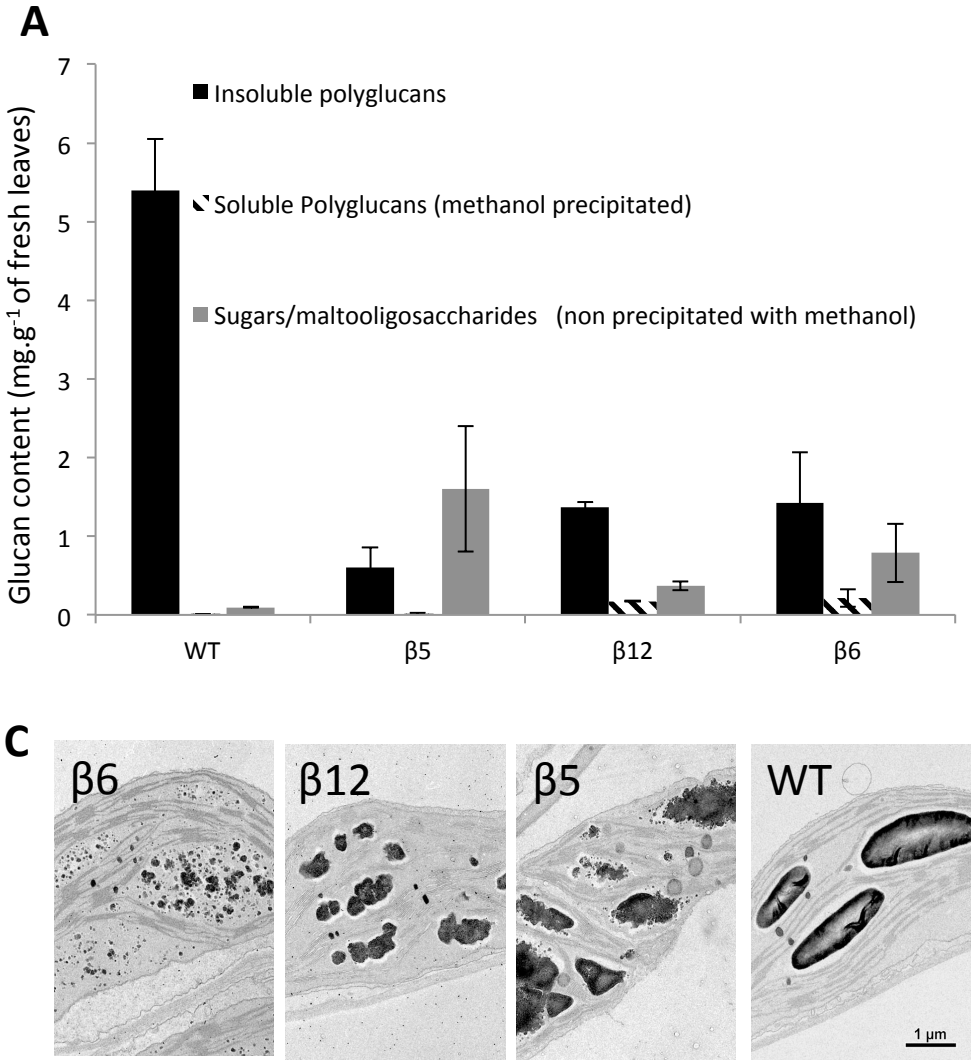


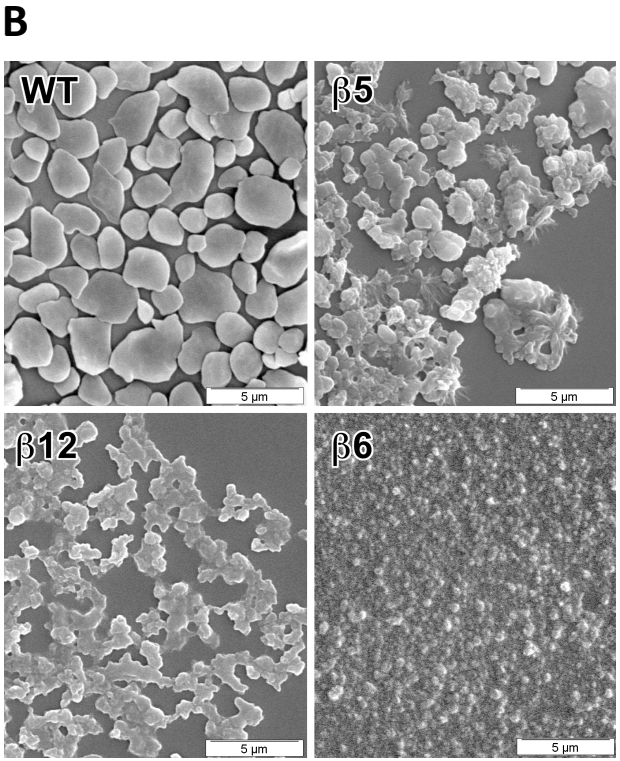


**Supplemental Figure S8 : Leaf glucan contents and granules morphology.**

A: For glucan content the average of three independent cultures are presented. Vertical thin bars are the standard deviation of three independent biological replicates. B: Scanning electron microscopy images of purified insoluble polyglucans. C: Transmission electron microscocopy images of leaf chloroplasts positively stained with PATAg.